Ecological Modelling 308 (2015) 45–62

Contents lists available at ScienceDirect

Ecological Modelling

journal homepage: www.elsevier.com/locate/ecolmodel

An integrated modeling approach for elucidating the effects of different management strategies on Chesapeake Bay oyster metapopulation dynamics

Michael E. Kjelland[a], Candice D. Piercy[a], Tahirih Lackey[a], Todd M. Swannack[a,b,*]

[a] U.S. Army Engineer Research and Development Center, Vicksburg, MS 39180, USA
[b] Department of Biology, Texas State University, San Marcos, TX 78666, USA

ARTICLE INFO

Article history:
Received 7 January 2015
Received in revised form 20 March 2015
Accepted 22 March 2015

Keywords:
Integrated environmental modeling
Oyster
Metapopulation
Spatially-explicit
Agent-based
Hydrodynamic

ABSTRACT

Eastern oyster abundance is at an all-time low, yet this species is a key component of many estuarine systems because it contributes to ecosystem function by providing habitat, improving water quality, stabilizing benthic and intertidal habitat, increasing landscape diversity and producing more oysters. Given the breadth of environmental benefits oysters provide, as well as their commercial and cultural importance, sustainable oyster production has become a priority in several regions, including the Chesapeake Bay. Current strategies include treating restored reefs as permanent sanctuaries, which provide long-term environmental benefits yet removes them from the fishery, or harvesting reefs on a rotational basis, which provides economic value yet decreases environmental benefits. The long term dynamics of these strategies is unknown. Oysters have a complex, biphasic life cycle (i.e., sessile adult and motile larval stages) and their viability is intimately tied to a suite of environmental factors including, but not limited to, flow regime, total suspended solids, temperature, salinity, and dissolved oxygen. In order to determine how different oyster management strategies affect oyster dynamics, we developed a multi-model approach that integrates a 2-D hydrodynamic model, a larval transport model, and a spatially-explicit, agent-based population dynamics model to simulate long term oyster dynamics. We applied our model to a ten reef system in the Great Wicomico River in the Chesapeake Bay, and simulated six different combinations of sanctuary and/or harvest management scenarios over an 8-year period. We evaluated the environmental and commercial benefits of each strategy. Our results indicated that sanctuary reefs are beneficial, and that the spatial position of sanctuary reefs strongly affected source-sink dynamics and must be considered before implementing a harvest regime. Simulations that did not consider the source/sink dynamics of the reefs yielded larger numbers of oysters for harvest in the short-term, yet resulted in a complete fishery collapse in the long term. Selective, rotational harvest, resulted in lower annual yield, but the fishery persisted throughout the eight year simulation. This integrated modeling approach helped reduce uncertainty within the study system and can help natural resource managers understand ecosystem-level processes leading to more informed decision making across spatial and temporal scales.

Published by Elsevier B.V.

1. Introduction

Oysters are reef forming organisms that provide critical ecosystem services to estuarine systems, including water quality improvements (Newell et al., 2002; Kellogg et al., 2013), landscape diversity (Eggleston, 1999), storm surge protection (Meyer et al., 1997; Piazza et al., 2005), habitat for reef-dwelling and benthic communities (Coen et al., 1999; Posey et al., 1999; Tolley and Volety, 2005), among others (Powers et al., 2009; Harding et al., 2010). Economically, oysters are a major fishery, with more than 100,000 metric tons harvested annually. Oyster abundance is currently at an all-time low, estimated at 15% of historic levels worldwide (Beck et al., 2011), and one percent within the Chesapeake Bay in North America (Rothschild et al., 1994; Kirby, 2004). A combination of anthropogenic factors (e.g., overharvesting and hydrologic modifications) and intense ecological interactions (e.g., increased instances of disease and predation) are thought to have caused the decline (Beck et al., 2011).

Over the last two decades oyster restoration has been a major focus of local, state and federal agencies, with the main objectives of restoration being to maximize environmental benefits, or

* Corresponding author at: U.S. Army Engineer Research and Development Center, Vicksburg, MS 39180-6199, USA. Tel.: +1 6016342068.
E-mail address: todd.m.swannack@usace.army.mil (T.M. Swannack).

http://dx.doi.org/10.1016/j.ecolmodel.2015.03.012
0304-3800/Published by Elsevier B.V.

maximize the yield from the fishery. Progress has been slow, due to economic cost, and to differences in how to interpret success, given the differing points of view from economic and ecological perspectives (Mann and Powell, 2007). Ultimately, however, the goals of the two groups are fundamentally similar, specifically, increase oyster abundance closer to historical levels so that oyster populations are self-sustainable and therefore maintain their ecological and economic footprint for the future.

The Chesapeake Bay oyster populations are managed by the U.S. federal government and the states of Maryland and Virginia (the bay sits on the border of these states). On the Virginia side of the bay, oyster management is focused on two major strategies: the creation of permanent sanctuaries (Schulte et al., 2009), which remain unharvested/unmolested in perpetuity, and rotational harvest, where individual reefs are harvested on a prescribed frequency, generally once every three years. The former strategy is thought to maximize environmental services including recruitment from the sanctuaries to harvested reefs, whereas the latter maintains the fishery while providing some environmental benefits during non-harvest years. It is currently unclear how these techniques affect the long term trends in oyster dynamics.

Oysters have a complex, biphasic life cycle which involves a planktonic larval stage and a sessile adult stage, which makes it difficult to study long-term population dynamics in the field. The viability of each life stage is intimately tied with specific ranges of local and regional environmental conditions, such as freshwater inflow, salinity, temperature, substrate condition, carbonate composition of sea water, among others. Flow patterns not only deliver food resources (oysters are sessile filter feeders which depend on flow patterns to deliver food), but also transport planktonic oyster larvae throughout the system. The concentration of TSS and phytoplankton varies spatially and temporally due to changes in environmental conditions such as freshwater inflows, temperature, light, nutrient concentrations, and flow dynamics caused by tide cycles, storm systems, wind patterns, etc. Likewise, determining how the population dynamics and productivity of sanctuary reefs differ from commercially harvested reefs, particularly those that are under rotational harvesting, is also complex due to the multiscale interactions among the physical, ecological and socio-economic factors.

The complexity of the oyster system facilitates developing ecological models to explore and forecast population dynamics, and there have been numerous studies that have modeled oyster population trends. Some of the earliest models focused on capturing the general aspects of oyster population dynamics (Hofmann et al., 1992, 1994; Powell et al., 1992, 1994, 1995), or their response to disease (Hofmann et al., 1995; Powell et al., 1996). More recent models have applied integrated environmental modeling techniques and combined multiple models, generally some combination of GIS, food web, hydrodynamic, larval tracking, and/or population models, to better capture the complexity found in the natural system. These models have focused on how oysters respond to environmental change (Dekshenieks et al., 2000), gene flow through metapopulations (Munroe et al., 2012), disease resistance (Powell et al., 2011, 2012), or restoration strategies (North et al., 2010). However, few studies have focused on the dynamics of sanctuary reefs, and to our knowledge, none have focused on the impact of sanctuary reefs at local and regional scales over long time periods, or how sanctuaries and rotational harvesting strategies compare to each other within the Chesapeake Bay.

In this paper, we first describe the Chesapeake Bay Oyster Population Model (CBOPM), an integrated hydrodynamic-larval tracking-population dynamics model, developed to aid in projecting future population trends for the eastern oyster (*Crassostrea virginica*) in the Great Wicomico River of the Chesapeake Bay. We evaluate the CBOPM by comparing model results to observed field data or other studies of *C. virginica* in the Chesapeake Bay. Finally, we apply the model to six different management strategies, using different combinations of sanctuary and rotational harvesting, to determine which scenarios provide sustainable solutions for the oyster fishery in the Great Wicomico River.

2. Model descriptions

2.1. Purpose

The CBOPM is designed to simulate oyster population dynamics for an 8-year period using an integrated hydrodynamic-ecological modeling approach. The model was designed to test how population dynamics and system-level biomass of the eastern oyster within a ten-reef system of the Great Wicomico River is affected over time by different management strategies.

2.2. Model overview

The CBOPM was conceptualized to capture the critical processes affecting the population dynamics of ten reefs of eastern oysters (*C. virginica*) within the Great Wicomico River of the Chesapeake Bay (Fig. 1), and consists of three models: 2-D Adaptive Hydraulics (ADH) for hydrodynamics, a Lagrangian Particle Tracking Model (PTM) for larval transport, and a spatially-explicit, agent-based population dynamics model (PDM) (Fig. 2). ADH and PTM have been documented elsewhere, and only the information pertinent to this study is reported, whereas the PDM was custom designed for this effort and is thoroughly described, following the protocol for agent-based models suggested by Grimm et al. (2010).

ADH provides daily hydrological factors that interact with reef dynamics, specifically, changes in the ebb and flow of tides, sediment transport, currents created by freshwater inflow regimes and associated suspended sediment transport or TSS, salinity, dissolved oxygen (DO), and temperature are factors accounted for by ADH and affect the following: reproduction, movement of oyster larvae and spat setting, growth and survival of individual oysters. ADH is described in Section 4.1.

The PTM is a modified Lagrangian particle tracking model originally developed for tracking sediment particles (MacDonald et al., 2006; Lackey et al., 2012). The particle tracking model was adapted for tracking biological particles by applying behavior rules that can supersede physical rules developed for inanimate transport (e.g., larval fish behaviors, Tate et al., 2010). In this work, PTM was further modified to specifically simulate behaviors of oyster larvae. The oyster larval transport modeling method is described in Section 4.2.

The PDM is a spatially explicit, agent-based, stochastic, simulation model, programmed in NetLogo v.5 (Wilensky, 1999) and it simulates oyster growth, reproduction, and mortality for oyster agents (oyster agents are treated as super-individuals, with each agent representing 100,000 oysters) on a daily time-step for 10 geo-referenced reefs in the Great Wicomico River (Fig. 1B). Individual oyster agents can only be located on reefs, which are distinct patches in the environment. Oyster population level patterns captured by the model include biomass, density, and average shell size for given age-cohorts, as well as larvae production and spat set locations. The population dynamics model is described in Section 4.3.

2.3. Entities, state variables, and scales

The CBOPM is driven by several environmental parameters that are generated by the ADH code (Table 1a) that are used as input for the PTM and PDM.

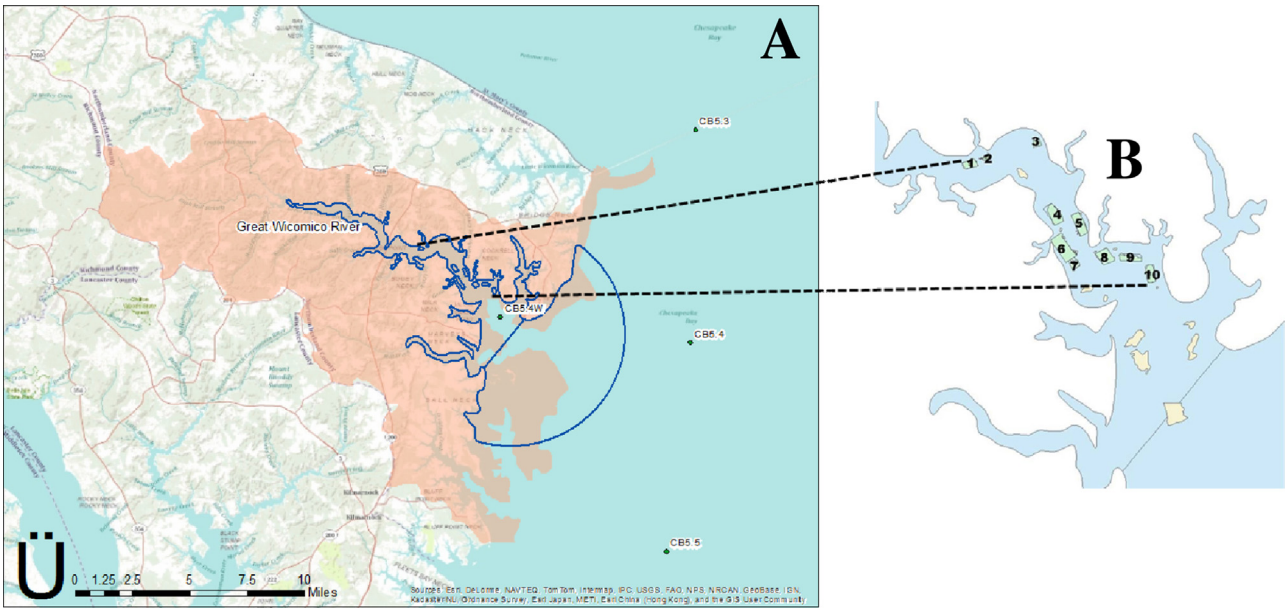

Fig. 1. Map of Great Wicomico River watershed and ADH model domain. (A) Orange shaded area is the watershed drainage area, blue outlined area is ADH model boundaries and material types, and green points are Chesapeake Bay Program long term monitoring stations; and (B) enlarged view of locations of 10 geo-referenced oyster reefs used for larval tracking and population dynamics models. Reefs are numbered for simplicity. (For interpretation of the references to color in this figure legend, the reader is referred to the web version of this article.)

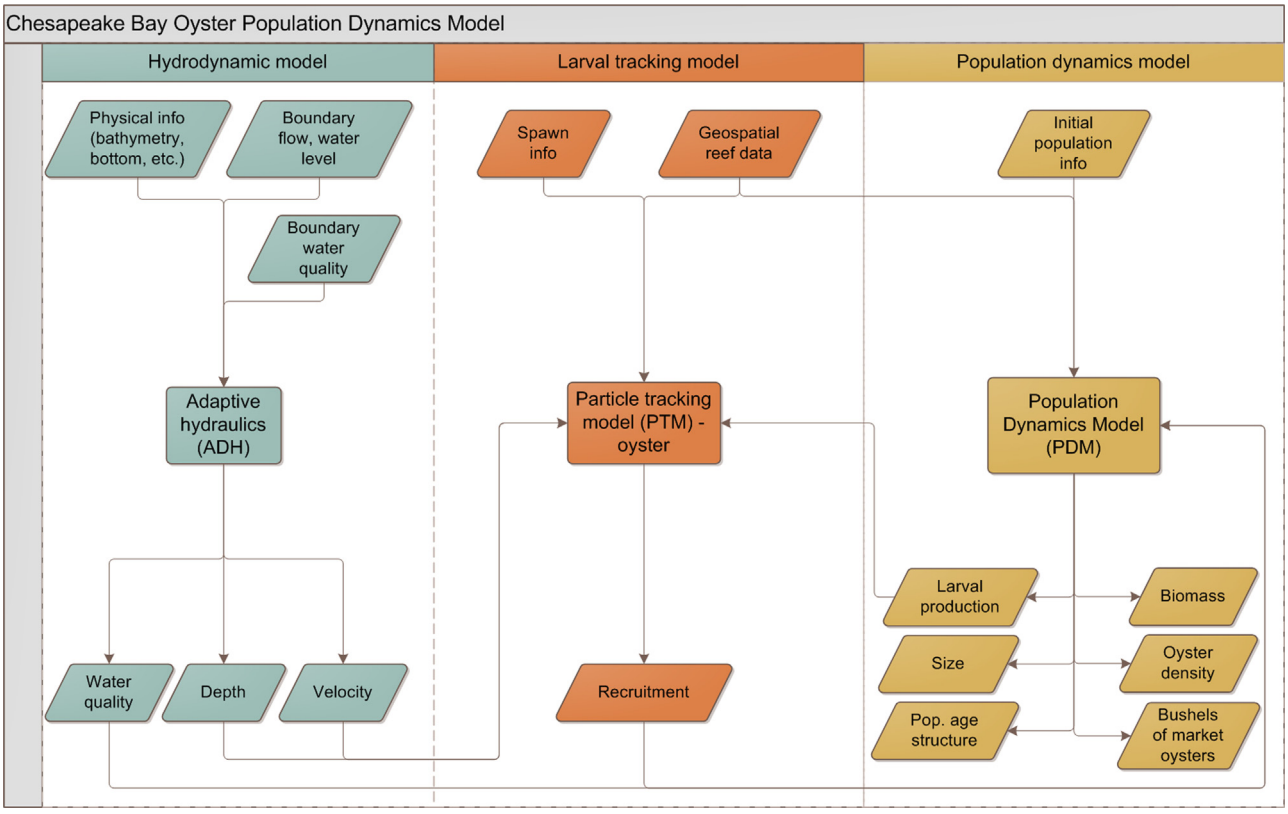

Fig. 2. Conceptual model of the integrated Chesapeake Bay Oyster Population Model (CBOPM). CBOPM consists of three models: a hydrodynamic model (left panel), Larval tracking model (middle panel) and a spatially-explicit agent based population dynamics model (right panel). Initialization requirements are along the top row, the specific models used are located in the middle, and the bottom row represents the outputs of each model. Arrows indicate the directions of input/output linkages among the models.

The PTM provides the PDM with connectivity matrices that determine the probability of intra- and inter-reef recruitment.

The PDM is composed of two classes (low-level entities): oysters and habitat patches. Oysters are described by 5 population parameters (Table 1b) and 13 state (low-level) variables (Table 1c). Collectives are represented in the model as specific, geo-referenced reefs (oysters located in a specific location that are separated from others) and age cohorts defined as the following: Spat/juvenile (0–1 years old), sub-adult (1–2 years old), adult (2–3 years old), 'adult +' (3+ years old). Habitat patches are described by 6 state

Table 1
Overview of oyster model components including: (a) input variables and environmental parameters, (b) demographic parameters, (c) attributes of the oyster class, (d) attributes of the habitat class, and (e) aggregated system-level variables.

Parameter	Value (status/unit of measure)
(a) Input & environment	
Spatial scale	16,641 patches (~30 m^2/patch)
Time step	1-day
Length of simulation	8 years
Depth[a]	m
H_2O temperature[a]	°C
Temperature duration	No. of days within temperature thresholds
Salinity[a]	ppt
Salinity duration[a]	No. of days within salinity thresholds
Total suspended solids[a]	mg/L
TSS duration[a]	No. of days within TSS thresholds
Dissolved oxygen (DO)[a]	mg/L
DO duration	No. of days within DO thresholds
Number of reefs[b]	10
Initial oyster biomass	No. of kilograms (lbs)/m^2
Initial oyster density	No. of oysters/m^2
(b) Demographic parameters	
Larval dispersal[c]	
Age at first reproduction	1 year
Stage specific mortality	Probability (Section 4.3.6)
Fecundity	Spat/female (Section 4.3.4)
Reproduction	Probability (Section 4.3.4)
(c) Attributes of agent class	
Status	Alive, dead
Identity	identification no.
Age	Years (0–3+, max. 10)
Life stage	Spat/juvenile, sub-adult, adult, & 'adult+'
Sex	0 = Male, 1 = Female
Size (total shell growth)	Length (mm)
Shell gain (daily shell growth)	Length (mm)
Energy reserves (expenditure of 1.2 unit/day)	max. = 8 unit
Energy acquired (influenced by environment)	max. gain = 2.8 unit/day
Biomass[d,e]	Grams (wet, dry, ash free)
Location of natal reef	Reef No.
Reproductive Status	Available, unavailable
Current reef location	Reef No.
Patch state variables	
(d) Description	
Spatial location	*X–Y* coordinate
ID No.	Identification number of reef
Reef substrate	present, absent
Reef type	low-relief, high-relief (Section 4.3.7)
Oyster biomass	No. of kg/m^2
Oyster density	No. of oysters/m^2
System-level variables	
(e) Aggregated variables	
Adult oysters ≥3 yrs old	No. of individuals
Adult oysters 2 yrs old	No. of individuals
Sub-adult oysters	No. of individuals
Spat/juvenile oysters	No. of individuals
Total population size	No. of individuals
Proportion 'adults+'	$0 \leq \# \leq 1$
Proportion adults	$0 \leq \# \leq 1$
Proportion sub-adults	$0 \leq \# \leq 1$
Proportion spat/juvenile	$0 \leq \# \leq 1$
Size (total system & per reef)	Length (mm)
Biomass (total system & per reef)	No. of Pounds
Oyster density (total system & per reef)	No. of individuals/m^2

[a] Input data from adaptive hydraulics model (see Section 4.1).
[b] Data provided by U.S. Army Corps of Engineers, Norfolk District.
[c] Input data from larval transport model (Section 4.2).
[d] Ash free dry mass equation from Whyte et al. (1990), Pouvreau et al. (2006)
[e] Ash free dry mass equation from Wang et al. (2008).

(low-level) variables (Table 1d). The model also includes 12 aggregated (system-level) variables (Table 1e). The values of all aggregated variables and status or values of all oyster state variables, except natal reef, potentially change during each simulated time step. Status or values of all habitat patch state variables, except reef location, potentially change during each simulated time step. The model simulates the population dynamics and movement with regard to oyster reef colonization or re-colonization over an 8-year period in 2920 one-day time steps. Each of the 900 habitat patches represents a ~30 m by ~30 m area of the Great Wicomico River.

2.4. Process overview and scheduling

The CBOPM proceeds in daily time steps to allow discrete events and processes to occur. Environmental parameters (Temperature (°C), Salinity, TSS (mg/L), and DO (mg/L)) are generated by ADH and used as inputs into the PDM. PTM provides reef-to-reef connectivity matrices on an annual basis (one 10×10 matrix per year) with the elements of the matrix representing the probability of larval particles that settle on each respective reef.

Initialization of the population dynamics model begins by importing ADH and PTM outputs, geo-referenced shapefiles, and initializing the oyster class (Fig. 2). Then the simulation proceeds by iterating through a series of 6 sub-models that (1) determines if oysters should advance to the next life stage (Section 4.3.2), (2) determines daily oyster growth based on current environmental conditions (Section 4.3.3), (3) calculates the reproductive dynamics and larval settlement, if appropriate (Sections 4.3.4 and 4.3.5), (4) calculates natural mortality (Section 4.3.6), (5) calculates management related mortality, if appropriate (Section 4.3.7), and (6) updates habitat patch state variables, aggregated variables and environmental parameters (Section 4.3.8). Within sub-models 2 through 4, all "alive" oysters are processed in a random order, and oyster state variables are updated as changes occur.

3. Model design—Design concepts

3.1. Basic principles

The CBOPM was designed to capture the critical processes affecting the oyster population within the Great Wicomico River, including hydrodynamics, larval transport, and life history of the oysters themselves. CBOPM is driven by ADH, which simulates water level, current velocities, and the environmental parameters which are used as input data for the PTM and PDM. Reef-to-reef recruitment dynamics were calculated based on results from the PTM, which was based on North et al. (2006, 2008). The population dynamics model draws upon the metapopulation concept (Levins, 1969), where each reef represents a distinct patch where colonization occurs via larval dispersal, thereby allowing the model to capture colonization and extinction events for individual reefs over a spatial and temporal context. Oyster growth was parameterized as a dynamic energy budget model developed by inverse modeling daily growth to approximate mean age-cohort sizes based on data from field studies and the scientific literature (following methods described in Grimm et al. (2005), and references cited therein).

3.2. Stochasticity

In PTM, particles are released at a random location within a prescribed volume above each oyster reef (source polygon). Particle movement is dictated stochastically based on the logarithmic velocity distribution (assumed for two-dimensional hydrodynamic model inputs), advective movement from near-bed turbulence, and

horizontal and vertical diffusion. In PDM, reproduction and mortality are all probabilistic and based on empirical estimates described in detail in Sections 4.3.4 and 4.3.6, respectively.

3.3. Collectives

There are two kinds of collectives represented in the model. First, oysters are defined as belonging to age cohorts (depending on specific ages of individual agents), each with their own attributes. We consider oysters of the same age to be in the same cohort, but each individual experiences its local environment independently and local conditions control growth, reproduction and mortality. Second, oyster reefs are aggregates of individual oyster agents at a particular location (Fig. 1). Reefs are spatially-discrete patches that contribute larval recruits to other reefs, and can have management actions assigned to them.

3.4. Observation

For ADH calibration, a time series of model-generated salinity values was compared to observed values from a Chesapeake Bay Program long-term monitoring station in Ingram Bay at the mouth of the Great Wicomico River. PTM behaviors were observed to ensure each behavioral process was coded correctly and provided reasonable results, and intra-reef recruitment values were compared to existing studies. For the population dynamics model, the interactions of oysters and their environment were observed process by process. For model analysis, only population-level variables were recorded, specifically, biomass, number of market-sized bushels, size and age class distributions, and overall abundance.

4. Sub-models

4.1. Adaptive hydraulics (ADH)

The CBOPM is driven by the ADH hydrodynamic model which simulates water level, current velocities, and constituent transport in the system of interest. ADH is an unstructured finite-element hydrodynamic modeling system that has been thoroughly documented in other studies (Danchuk and Wilson, 2010; Horner et al., 2010; Pettway et al., 2010; Tate et al., 2012; Savant and Berger, 2012; McAlpin et al., 2013; Martin et al., 2012). The focus here is on discussing how we developed an ADH simulation for the Great Wicomico River to provide water level, current, and water quality data to the population dynamics model and the PTM. ADH can simulate saturated and unsaturated groundwater, overland, three-dimensional Navier–Stokes, and two- and three-dimensional shallow water flows. The two-dimensional shallow water flow implementation was used in this application since the Great Wicomico River is relatively well-mixed and the spatial precision and simulation period required for this particular problem would make a more computationally intensive implementation of ADH unfeasible. The model inputs are the physical geometry of the system, upstream and downstream boundary conditions, and meteorological conditions. The model outputs are the depth-averaged velocity and depth and the constituent concentration at each node.

The Great Wicomico River bathymetry was derived from bathymetric surveys conducted by NOAA and USACE at resolutions ranging from 1- to 30-m. All survey data were converted to the NAVD88 vertical datum and re-sampled such that the highest resolution data were used where available and lower resolution data were used to fill in any gaps. The boundary of the ADH mesh was set at the −0.5-m topographic line (NAVD88) to minimize wetting and drying behavior within the model. Bottom roughness was calculated using the Manning's equation and with an assumed Manning's n of 0.02. The resulting ADH mesh contained ~25,000 triangular elements constructed from ~14,000 nodes with spacing ranging from approximately 40 m to 335 m, with finer resolution occurring over the oyster reefs and areas with highly variable geometry such as slope breaks, mouths of tributaries, and sharp bends (Fig. 3).

The bayward boundary was assumed to be semi-circular with the eastward edge located near the CB5.4 water quality monitoring station (Fig. 1). The bayward boundary was defined by an hourly tailwater elevation using a harmonic tide. Average temperature, salinity, TSS, and DO along the boundary was calculated from a linear spatial interpolation between the long-term monitoring stations CB5.3, CB5.4, and CB5.5; only measurements from the surface zone were used as the water in the Great Wicomico River and Ingram Bay most closely resembles the surface zone of the Chesapeake Bay.

The upstream boundary of the model domain and the lateral inflows along the coastline was defined by a daily discharge at each tributary with a drainage area greater than two square km. The only USGS stream gage in the Great Wicomico River watershed is at Bush Mill Stream. The period of record for this gage extends from 1963 to 1987. The closest gaged stream with similar watershed characteristics (drainage area, land use, and topography) and with a period of record overlapping the model study period is Dragon Swamp in the Piankatank River watershed, which is one river system to the south of the Great Wicomico River. The daily inflow at each tributary stream for the simulation period was estimated by multiplying discharge at Dragon Swamp by the ratio of the mean annual flowrate of Dragon Swamp in the NHDPlus Version 2 data set (2012). The NHDPlus Version 2 data set uses multivariate regression equations developed in Vogel et al. (1999) to estimate the mean annual flowrate based on watershed characteristics including geographic location, area, temperature, and precipitation.

The dissolved oxygen of the fresh water entering the Great Wicomico River was assumed to be at saturation. Monthly average water temperature was applied to the freshwater inflows as calculated from the 1963–1987 Bush Mill Stream period of record. Lateral inflows were assumed to have 0 ppt salinity and 0 mg/L TSS, which is consistent with the Chesapeake Bay Estuary model assumptions (Cerco and Cole, 1993) and deemed reasonable given the lack of data. Inputs due to bank erosion were not considered.

Water surface fluxes were calculated across the surface of the model domain by calculating the net daily precipitation and/or evaporation using precipitation data from the nearest National Climactic Data Center weather station at Walkerton, VA (http://www.ncdc.noaa.gov/) with a complete record for the model simulation period and evaporation data from the Objectively Analyzed Air–sea Fluxes (OAFlux, http://oaflux.whoi.edu/index.html) project for the latitude-longitude of the Great Wicomico River. Wind effects are included in ADH; the Teeter method for shallow water was used to calculate the surface stress from wind (Teeter et al., 2001). Hourly wind data from the nearest NOAA weather stations (Lewisetta, VA and Rappahannock Light, VA) with a period of record that corresponded with the simulation period were applied uniformly across the model domain.

The ADH model was calibrated for 2005 using monitoring data at the CB5.4W monitoring station in Ingram Bay. ADH has few calibration parameters; in this simulation, eddy viscosity and Manning's roughness were adjusted to most closely match conditions at the CB5.4W long term monitoring station. Constituent diffusion is calculated from eddy viscosity. Eddy viscosity was calculated using the Smagorinsky method option in ADH (Smagorinsky, 1963) that accounts for anisotropic mixing relative to the direction of flow. Model element spacing and time step were also adjusted to provide a balance between spatial and temporal resolution and computational speed. For this application, mesh adaptation was not allowed

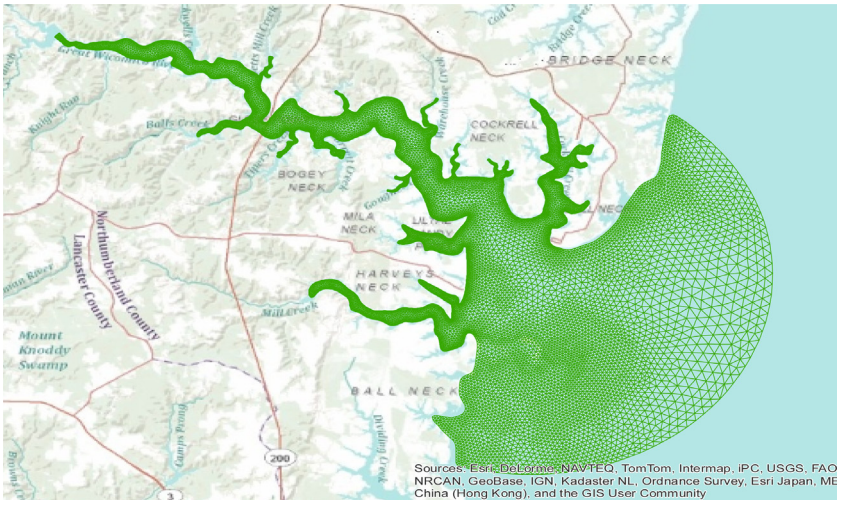

Fig. 3. ADH mesh for the Great Wicomico River. There are approximately 25,000 triangular elements constructed from 14,000 nodes with spacing ranging from approximately 40 m to 335 m. The finer spatial scale occurs over the oyster reefs and in areas where more resolution was needed to solve the hydrodynamic equations.

as model runtime was a concern given the length of the simulation period.

The calibrated model was run for an 8-year simulation (2005–2012) through the 2012 spawning season. The simulation period was chosen to correspond with the period during which active oyster restoration occurred within the Great Wicomico River.

4.2. Larval transport modeling using PTM

Oyster recruitment occurs through the settlement of larvae released from that reef (intra-reef recruitment), or from other reefs within the system (inter-reef recruitment). Oyster larvae have limited swimming abilities so their movement is controlled in large part by hydrodynamic transport. Oyster larvae have a maximum swim speed on the order of 2 to 3 mm/s (North et al., 2006, 2008), which is negligible in comparison to the horizontal velocities typically observed in most estuarine systems. However, vertical velocities are much lower, and veligers are able to overcome vertical velocity gradients to change their vertical position in the water column.

Langrangian particle tracking models can be adapted for tracking biological particles by applying behavior rules that can supersede physical rules (e.g., Tate et al., 2010) successfully modified PTM to simulate various characteristic larval fish behaviors in the Mississippi River Gulf Outlet). As a Lagrangian particle tracking model, PTM uses computed water level and velocity values from two- and three-dimensional hydrodynamic models to predict discrete constituent transport. The transport model is uncoupled from the hydrodynamic model, so multiple simulations using the same pre-computed hydrodynamics, may be run efficiently by varying input conditions such as the locations in which larvae will be introduced into the system. For each simulation time step PTM tracks the particle through the hydrodynamic flowfield, by interpolating the velocity from the nodes surrounding the particle to the exact particle location. These fundamental transport components of PTM were enhanced to predict oyster larvae transport by augmenting the model with algorithms which emulate biologically-based behaviors to simulate oyster larvae transport pathways within the system (Fig. 4). Veliger density and swimming ability changes with age, temperature, and salinity, so the basic behavior rules were simplified to best approximate the vertical distribution of veligers in a well-mixed system. We developed a rule set to achieve a temporally varying vertical distribution of veliger particles consistent with North et al. (2008). Our model differs from North et al. (2008) and Narváez et al. (2012) in that we used a higher resolution hydrodynamic model (ADH compared to ROM, with resolutions ranged from 40 m to 335 m (ADH) and from 200 m to 1 km (ROMS)), and was implemented in a different software suite. The finer resolution allows us to explore fine-scale patterns in larval transport and reef-to-reef connectivity, which is not possible with larger scale hydrodynamic meshes or grids. We specifically limited our case study to the Great Wicomico River, whereas North et al. (2008) simulated larval transport across the entirety of the Chesapeake Bay, but did not consider the Great Wicomico River.

Veliger particles were assumed to be neutrally buoyant when released near the water surface and advection was allowed to distribute the particles throughout the model domain. Once the veligers matured to age at which settlement could occur (assumed to be 14 days), they migrated to within one meter of the bottom where their movement was dominated by boundary layer processes until they came into contact with a suitable substrate for settlement. For this modeling phase, we assumed that oyster larvae could only settle on the ten modeled reefs (Fig. 1B), and no recruitment entered the system from outside the modeled reefs. Veliger particles that did not come into contact with reef areas between 14 and 21 days died.

To achieve the bimodal spat set observed in the Chesapeake Bay, five instantaneous particle releases were simulated (consistent with North et al. (2008). Autocorrelation analysis of shell string data for the Great Wicomico River (Southworth et al., 2006, 2007, 2008, 2009, 2010a, 2011, 2012) indicated spawning is triggered when temperatures at station CB5.4W reached 22 °C as opposed to the 25 °C assumed in the North et al. (2008) model. Ten replicates of each particle release were simulated and the average was reported to the population dynamics model as the veliger particle transport success rate. To estimate reef-to-reef dynamics, annual transport success among reefs was converted into a connectivity matrix (see below), which represented the probability average percentage of larvae that moved from $reef_n$ to $reef_x$ (where n is the nascent reef and x is one of the other reefs in the system, including n). Due to year-to-year fluctuations in flow dynamics a connectivity matrix is generated for each of the eight years simulated. These percentages are considered to be the probability of a given larvae settling on a specific reef during that specific spawning event. The below matrix represents reef-to-reef recruitment for reef 5 across the eight years of the simulation (e.g., 0.113

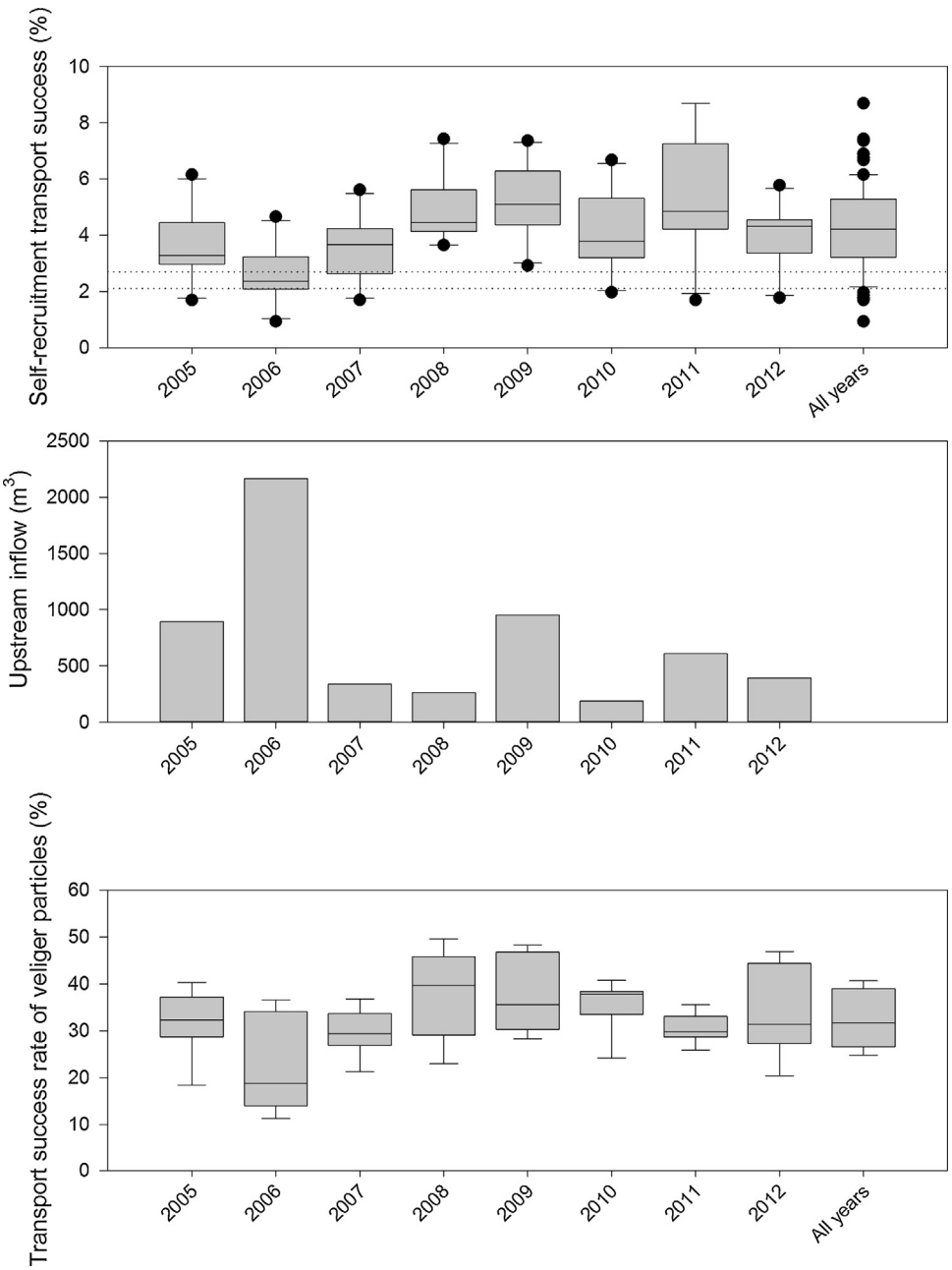

Fig. 4. (A) PTM self-recruitment across 8 years. Dotted lines indicate min and max rates from North et al. (2008) and dots represent statistical outliers; (B) summer freshwater inflow volume; and (C) transport success rate of veliger particles across 8 years.

represents the probability that larvae from reef 5 settle on reef 2 during the 1st year of the simulation, and 0.151 represents reef 5's self-recruitment for year 3). The PDM calculates veliger particle mortality separately; PTM was only used to calculate transport success.

4.3. Population dynamics model

4.3.1. Initialization and input data

Input for the population dynamics model include (1) eight years of hydrodynamic and environmental data from ADH, (2)

$$\begin{Bmatrix} & \text{reef}_1 & \text{reef}_2 & \text{reef}_3 & \text{reef}_4 & \text{reef}_5 & \text{reef}_6 & \text{reef}_7 & \text{reef}_8 & \text{reef}_9 & \text{reef}_{10} \\ \text{year}_1 & 0.060 & 0.113 & 0.056 & 0.194 & 0.105 & 0.079 & 0.079 & 0.133 & 0.046 & 0.135 \\ \text{year}_2 & 0.081 & 0.101 & 0.083 & 0.225 & 0.120 & 0.084 & 0.084 & 0.095 & 0.053 & 0.073 \\ \text{year}_3 & 0.090 & 0.098 & 0.104 & 0.203 & 0.151 & 0.070 & 0.070 & 0.088 & 0.051 & 0.076 \\ \text{year}_4 & 0.093 & 0.154 & 0.152 & 0.114 & 0.166 & 0.060 & 0.060 & 0.087 & 0.053 & 0.061 \\ \text{year}_5 & 0.063 & 0.107 & 0.091 & 0.104 & 0.166 & 0.068 & 0.068 & 0.112 & 0.092 & 0.131 \\ \text{year}_6 & 0.080 & 0.093 & 0.109 & 0.160 & 0.160 & 0.085 & 0.085 & 0.095 & 0.043 & 0.091 \\ \text{year}_7 & 0.010 & 0.028 & 0.017 & 0.038 & 0.037 & 0.030 & 0.030 & 0.038 & 0.031 & 0.052 \\ \text{year}_8 & 0.028 & 0.030 & 0.032 & 0.063 & 0.046 & 0.024 & 0.024 & 0.030 & 0.019 & 0.036 \end{Bmatrix}$$

reef-to-reef connectivity matrices for each year of the simulation generated by PTM, and (3) GIS shapefiles consisting of georeferenced reef locations for 10 reefs that are within the Great Wicomico River. Input files were imported as .CSV files, and shapefiles were provided by the U.S. Army Corps of Engineers Norfolk District (USACE-NAN). Oyster reefs were populated with oyster agents approximating the age- and size-class distribution from corresponding reefs in the Great Wicomico River (Schulte et al., 2009; refer to Tables 1–4 in the Supplemental material for exact values).

Three parameters for the dynamic energy budget were set at initialization: (1) number of units of stored energy reserves, assigned randomly from a uniform distribution with a max of 10 unit and min of 0, (2) energy acquired per day was initialized at 2.8 unit per day but is modified as the simulation proceeds on an agent-by-agent basis based on local environmental conditions, and (3) daily energy-expenditure is initialized as a fixed amount (1.2 unit/day). The values for initialization for the energy budget model are described in detail in Section 4.3.3 and in Table 5a–d in the Supplemental material.

4.3.2. Aging

Oyster age (in years) is advanced on the first day of each calendar year (1 January). There are four stages associated with yearly ages: spat/juvenile (age 0–1), sub-adult (age 1–2), adult (age 2–3), and 'adult +' (age ≥ 3). Age is recorded independently of any other variable.

4.3.3. Growth

Food intake/energy assimilated was variable and implicitly represented as a probabilistic function of the amount of energy obtained by individual oysters at any given time-step. Competition among oysters was assumed to be negligible, especially given that oysters are at about 1% of their historical population in the Chesapeake Bay (Newell, 1988; Jackson et al., 2001; Maryland Department of Natural Resources, 2009; Wilberg et al., 2011), and perhaps as low as 0.3% of the historical abundance (Wilberg et al., 2011). Likewise, it was assumed that an adequate food supply was available throughout the time period simulated because anthropogenic nutrient over-enrichment, i.e., agricultural fertilizer run-off and sewage inputs, has caused enhanced phytoplankton production along coastal margins (Shumway, 1990; Malone, 1992; Conley, 2000; Cloern, 2001; Newell, 2004). This assumption is a generalized, non-spatially oriented one given that very high densities and resultant competition for spatially limited resources can occur (e.g., Lohse, 2002), albeit most likely at a finite temporal scale.

A net energy mass balance approach, with energy assimilation (Table 5a–d in Supplemental material) and metabolism components under different environmental conditions, was incorporated into CBOPM (similar to the oyster anabolism and catabolism relationships within AquaShell™ (Ferreira et al., 2010). Such a generalized proxy captures the elements of energy flow dynamics in the oyster population, without specifically parsing the energy flow dynamics and thereby avoiding more detailed parameter requirements and assumptions such as allotted somatic tissue energy (i.e., energy ingested, adsorption efficiencies, anabolic/metabolic processes, energy not utilized and excreted in the form of pseudofeces, energy lost to respiration, versus energy allotted for reproduction requirements, all on a finite time scale). We also incorporated a size dependent growth rate adjustment to capture the dynamics of dampenend growth rates in older oysters (refer to Table 6 in the Supplemental material).

We calculated both wet and dry biomass. Biomass in grams of dry weight was calculated based on shell length, using the following equation from Southworth et al. (2010a,b)

$$\text{Biomass} = 9.6318 \times 10^{-6} \times \text{SL}^{2.743} \quad (1)$$

where Biomass represents grams of dry tissue and SL represents shell length in mm. Wet biomass (grams of wet tissue) was calculated from dry weight following Whyte et al. (1990) and Pouvreau et al. (2006) as follows

$$\text{WB} = (\text{Biomass} \times 5.6667) + \text{Biomass} \quad (2)$$

where WB is grams of wet tissue, and Biomass is grams of dry tissue.

Oysters are considered large enough for market at 76 mm (Chesapeake Bay Program, 1989; LRSC, 2004). A maximum size class of 320 to 325 mm was imposed to reflect the largest size that any oyster would be likely to attain (Kennedy et al., 1996;Volstad et al., 2007).

4.3.4. Reproduction

Reproduction is calculated as the number of spat that can successfully settle on either its natal reef or another reef in the system. Each year two reproduction windows are simulated: the first takes place between 22 and 28 July (days 203 through 209), and the second between 31 July and 2 Aug (days 212 through 214). Dates of settlement were based on data indicating that spawning can start in early June and is largely complete by the end of August (Kennedy and Krantz, 1982; Kennedy et al., 1995; Kimmel and Newell, 2007). We calculated overall spawning and recruitment patterns in the PTM (described in Section 4.2).

The age at first reproduction for eastern oysters is one to two years of age at 3.0 cm to 4.7 cm shell length (Galtsoff, 1930; Gosselin and Qian, 1997; Dew, 2002). Oysters mature at an early age (usually by an age of 1 year) (LRSC, 2004).

Reproduction occurs once oysters are at least 1 year of age, is stochastic and depends on energy reserves, age-class (size), reef density, and the daily values of salinity, TSS, temperature and DO For a given oyster agent, the total fecundity is calculated as

$$F_{\text{total}} = F \times F_{\text{adj}} \times \text{ER} \quad (3)$$

where F represents the base fecundity rate of 3 spat per female successfully settling (based on Volstad et al., 2007), F_{adj} represents the adjustment to the base fecundity rate, and ER is a binomial variable representing whether or not the agent has enough energy for reproduction (1 = True, 0 = False). PTM does not assume any larval mortality and calculates the overall proportion of larvae that would settle on a reef without mortality. F_{total} provides an estimate of settling after mortality.

Fecundity is directly related to the body size (Dew, 2002), and female eastern oysters in the Chesapeake Bay area can release from 4 to 9 million eggs (Cox and Mann, 1992). Oyster fecundity increases with size/age) (Cox and Mann, 1992; Dew, 2002; Schulte et al., 2009). However, overall fecundity can be affected by environmental conditions (Kennedy et al., 1996). For example, poor spat production occurs at salinities below 14 ppt (Shumway, 1996; Volety et al., 2009). We calculated the adjustments to the base fecundity rate as

$$F_{\text{adj}} = \min(E_i) \times F_{\text{age}} \quad (4)$$

$$F_{\text{age}} = \text{RDE} \times k \quad (5)$$

where $\min(E_i)$ is the minimum value of the effects of the four environmental parameters (salinity, TSS, temp, and DO) on fecundity. Each environmental effect is calculated as an index between 0 and 1, and is based on empirical estimates from the literature (refer to Table 7 and the section regarding calculating impacts of environmental variables on reproduction in the Supplemental material for a complete description of the environmental–reproduction interactions and the logic that we used to develop these values). F_{age} represents the age-specific effects on fecundity, which is affected by an agent's age, reef density (RDE), and the probability that an oyster of a given age is female (k).

Table 2
The effect of reef density (RDE) on age-specific fecundity values.

Oyster density (oysters/m^2)	Age			
	1	2	3	>3
≥200	0.5	1	1.5	2.25
<200	0.25	0.5	1	1.5

The effect of reef density on reproduction (RDE) was calculated by incorporating a density dependent feedback on age-specific fecundity similar to North et al. (2010) and Wilberg et al. (2011). Unlike those studies, we incorporated density of oysters as having an effect on fecundity to specifically capture any density dependence effects on reproduction within given reefs. Specifically, if the overall density of the breeding age oysters on a given reef was greater or equal to the density-dependence positive influence on fecundity value (200 oysters/m^2), then age-specific fecundity was increased. Conversely, if density was less than 200 oysters/m^2, overall fecundity was reduced. Refer to Table 2 for exact values. The change in reproductive potential per square meter over time is a function of temporal change in per-capita fecundity and oyster density and can result in an increase of ~400%, on average (Puckett and Eggleston, 2012; Mroch et al., 2012).

C. virginica is protandric and the probability of becoming female increases with age. During reproductive windows, we calculated the probability of a given agent being a viable, reproductive female based on age rather than assign permanent genders to a specific agent. More specifically, oysters that are younger than three have a probability of reproducing of 0.5, and those older than three have a probability of 0.75 (Volstad et al., 2007). Probabilities were drawn from a uniform random distribution between 0 and 1. If an oyster could reproduce k was assigned a value of 1; if not, k was 0.

4.3.5. Recruitment

Overall reproductive output per reef is aggregated and parsed among the reefs according the connectivity matrix generated by the PTM (Section 4.2). Each recipient reef receives the number of agents corresponding to the proportion of aggregated output from the donor reef. Once an agent is assigned to its reef, natal reef and settling reef are recorded to determine source-sink dynamics, and reef-to-reef connectivity.

4.3.6. Mortality

Daily oyster mortality is stochastic, stage-specific, and is controlled by four environmental factors: salinity, TSS, temperature, and DO. There is a considerable amount of uncertainty associated with the influence of each mortality factor on each life stage, particularly at daily timescales. Thresholds values and exposure durations are more common and wide ranges of values have been reported in the literature. To estimate the probability of daily mortality, we used upper and lower threshold values as the maximum and minimum boundaries to develop a series of step-functions, with the intermediate steps resulting from empirical estimates from the literature or quantitatively approximated from neighboring steps. Step functions were developed separately for single day events and durations (exposures lasting more than 1 day). During each time-step, we calculated the conditional probability of individual agents dying from salinity, TSS, temperature, and DO (refer to Table 8a-f in the supplemental material for the threshold values logic we used to calculate the mortality-environment interactions these values). We then used a pattern-oriented approach (e.g., see Grimm et al., 2005) to test several functional forms (linear, exponential, etc.) of each step function in order to determine which form realistically recreated the patterns of growth rates, stage-class distributions, abundance, biomass, and density of oysters observed in the field (based on Southworth et al., 2006, 2007, 2008, 2009, 2010a,b, 2011; Schulte et al., 2009). We also used the daily mortality rate of 0.0026 (Crockett et al., 2012) as a reference point for comparing if CBOPM-estimated mortalities were higher or lower than seemed reasonable. We did not model any interaction effects among the mortality-causing environmental factors.

In addition to the mortality factors mentioned above, oysters could also die from three other causes:

(1) If oysters have an energy balance of 0 and no energy reserves.
(2) If oysters cannot gain energy (i.e., feed) for 8 consecutive days (based on Shumway, 1996; Volety et al., 2009, Volstad et al., 2007).
(3) If oysters reach 10 years old. Oysters ≥10 years of age are considered to comprise a negligible, i.e., <0.5% of the population in the Great Wicomico River, so we assumed that the maximum age of a simulated oyster was 10 years (Galtsoff, 1964; Powell et al., 2011).

4.3.7. Management

At the beginning of each simulation, each reef density is initialized as either high-relief (HR) or low-relief (LR), with HR reefs having four times the density of LR reefs (terminology and concepts following Schulte et al., 2009). Each reef can be parameterized as a permanent sanctuary or available for harvesting. Sanctuary reefs are not harvested during the simulation, and their mortality rate is only affected by processes described in Section 4.3.6. Harvested reefs are parameterized as LR (which mimics traditional harvesting practices), then subjected to harvest at user-defined frequencies (e.g., once a year, once every 3 years, etc). Harvesting can occur simultaneously for all reefs, or can be staggered so a subset of reefs is harvested each year (e.g., on a three year rotation, reefs 1–3 can be harvested during years 1, 4, and 7; reefs 4–6 on years 2, 5, and 8, and reefs 7–10 on years 3 and 6, or any other combination). Harvesting is a form of mortality and permanently removes a user-specified percentage of oysters from each harvestable reef. Specific size classes can be harvested which captures the policies of the oyster fishery. Any oysters remaining on a reef after harvest are allowed to grow and reproduce normally until the next harvest event. In the CBOPM, harvest occurs on one day (Day 298, October 25) to reflect the harvesting season that occurs from October through March in the Chesapeake Bay.

4.3.8. Update habitat patch state variables, aggregated variables, and environmental data

This sub-model updates all habitat patch state variables (Table 1d), e.g., newly oyster reef repaired patches or recently harvested/removed reef patches due to reef management decisions, and aggregated variables (Table 1e) to reflect changes that occurred during the present time step. The habitat patch state variables are also updated based on the input data that are to be used for the next time step. Environmental variables are updated to reflect conditions for the next time step.

5. Model evaluation

5.1. ADH

ADH output was compared with conditions at the CB5.4W monitoring station in Ingram Bay for an 8-year period from 2005 to 2013 (Fig. 5). No water level or current data are available within the model domain, so calibration and validation were conducted based primarily on salinity and temperature. ADH accounts for the barotropic effects of salinity and temperature even in 2-D simulations so if salinity and temperature are adequately simulated, we assume that water level and currents are also adequately simulated.

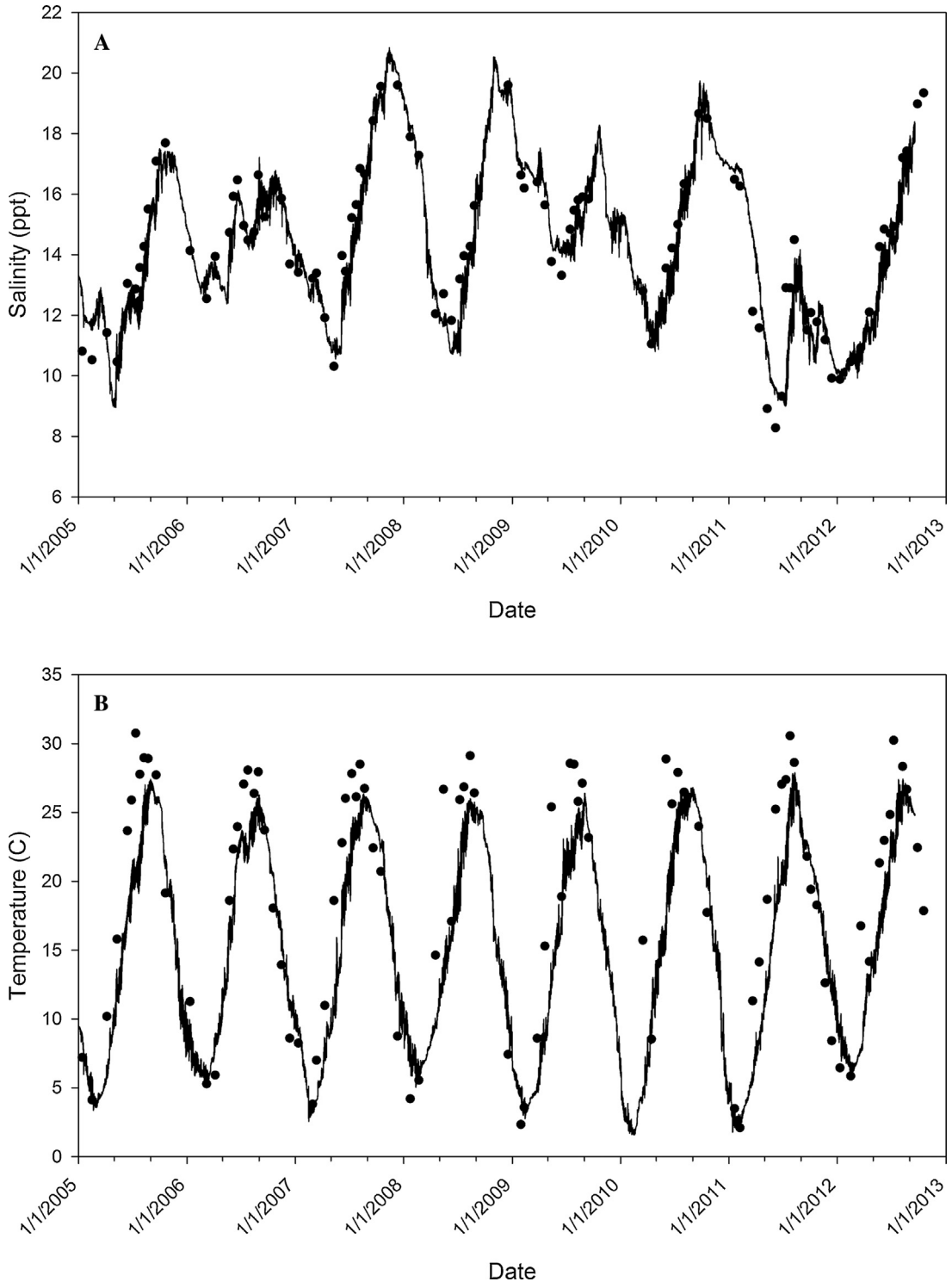

Fig. 5. Observed and ADH modeled values for (A) salinity and (B) temperature at CBP station CB5.4W. Points are observed data and the line is hourly ADH results.

Table 3
Goodness-of-fit statistics for ADH simulation of the Great Wicomico River system.

Goodness-of-Fit Statistic	ADH—2005–2012		ADH—2005		CH3D-ICM—2005	
	Salinity	Temperature	Salinity	Temperature	Salinity	Temperature
Nash–Sutcliffe model efficiency (NSE)	0.87	0.69	0.84	0.71	0.67	0.89
Root mean square error (RMSE)	0.92	4.75	0.93	4.86	1.35	2.91
Root mean square error-observations standard deviation ratio (RSR)	0.36	0.55	0.40	0.54	0.57	0.32
Percent bias (PBIAS)	−0.02	−0.13	−0.02	−0.16	0.02	−0.04
Index of agreement	0.97	0.91	0.95	0.91	0.88	0.97

Generally, ADH captures the patterns of salinity changes over the modeled period relatively well (Fig. 5A). Lower salinities tend to be over-predicted but the goodness-of-fit statistics (Table 3) do not indicate a strong tendency towards bias; with a percent bias of only about 1.5%. Using the general model performance ratings developed by Moriasi et al. (2007), a Nash–Sutcliffe Efficiency of 0.87 and a root square ratio of 0.36 for ADH salinity predictions indicate very good model performance. ADH does not capture the temperature dynamics within the Great Wicomico River as well as the salinity dynamics (Fig. 5B). ADH tends to under-predict summer water temperatures although it captures the seasonal variability fairly well. The goodness-of-fit statistics for temperature reflect the difference in model performance; the lower Nash–Sutcliffe Efficiency of 0.69 and root square ratio of 0.55 achieves a good model performance rating.

5.2. PTM

PTM produces a veliger particle transport success rate which must be combined with a veliger particle mortality rate dependent upon simulated local water quality conditions to provide an estimate of recruitment rates. In the PDM, recruitment is a function of the recruitment rate as well as current oyster age distribution and abundance, and water quality conditions during the spawning period. As the PTM only calculates transport success rates (not recruitment) and includes only a subset of oyster reefs, the raw PTM results cannot be directly validated with field data.

However, given the importance of understanding reef-to-reef connectivity in oyster systems, we compare our results with North et al. (2008) and Narváez et al. (2012) to provide assurance that our results are consistent with recruitment and transport patterns observed in the Great Wicomico River and the Chesapeake Bay in general. North et al. (2008) calculated self-recruitment rates—the rate at which veliger particles originating from a reef return to the same reef. Self-recruitment rates ranged from 2.1% to 2.7% for the years 1995 to 1999. The PTM self-recruitment rates for the Great Wicomico River tend to be higher with the median rates ranging from 2.3% to 5.0% (Fig. 4A). Our settlement rates fell within the ranges reported by Narváez et al. (2012). This pattern actually reflects observed higher recruitment rates within the Great Wicomico River (Southworth et al., 2006, 2007, 2008, 2009, 2010a,b, 2011). The mean dispersal distance for veliger particles correlates with river size with lower dispersal distances in smaller river systems (North et al., 2008). Given the small size of the Great Wicomico River, we can assume that most veliger particles would settle relatively close to their origin reef-likely within the Great Wicomico River rather than reefs in the mainstem Chesapeake Bay. North et al. (2008) also found mean dispersal distance as well as self-recruitment rates were influenced by freshwater inflow during the spawning season with higher summer inflows leading to repressed recruitment. Our results are consistent with those of North et al. (2008) showing reduced veliger particle transport success and self-recruitment during years with higher summer inflow volumes (Fig. 4B). While our overall veliger particle transport success rates were lower than North et al. (2008) who reported values between 66 and 71% (Fig. 4C), we can attribute that to the set-up of suitable substrate in each model. We only allowed settlement on the ten simulated reefs in CBOPM while North et al. (2008) allowed settlement on any historical oyster ground providing much larger areas for potential settlement.

5.3. Population dynamics model

We evaluated the usefulness of the CBOPM for projecting population dynamics of the eastern oyster in the Great Wicomico River by comparing patterns of (1) simulated oyster lengths to field data collected within the Chesapeake Bay, (2) simulated oyster densities to field density estimates collected from the Great Wicomico River, (3) simulated biomass to field samples collected from the Great Wicomico River, and (4) simulated age class distributions to field samples collected within the Great Wicomico River. For evaluation, we ran 25, 8-year, Monte Carlo (replicate stochastic) simulations. We parameterized the model to represent the habitat and historical environmental conditions within the Great Wicomico River from 2005 to 2012, which included two HR reefs and eight LR reefs, Simulated oyster lengths followed trends observed in other studies (Fig. 6A). Simulated growth rates were reasonable although larger oysters (i.e., $\geq$80 mm) were at or slightly above the recorded values for the Chesapeake Bay and the Great Wicomico River (Fig. 6B). These larger values may in part be due to the lack of fine resolution TSS and DO effects that could further reduce growth rates, or a result of larger oysters not being present in the real system due to over 100 years of harvesting. Harvesting (and/or poaching) appears to reduce mean shell height by removing market-sized oysters as the population matured to a harvestable size range; as a result, size at age estimates in the study were likely underestimated (Coakley, 2004; Paynter et al., 2010). Simulating more high-relief sanctuary reefs will skew the average oyster sizes towards larger size classes, whereas in the real system harvest/poaching effectively reduces the size; the same case may be made for oyster densities, oyster biomass, and age class distributions.

Simulated growth rates per age class fell within the values reported by Coakley (2004) and Schulte et al. (2009) (Fig. 6B). Simulated age class distributions were similar to field collected samples within the Great Wicomico, based on data from Schulte et al. (2009) for HR and LR reefs. High-relief reefs and low-relief reefs typically had a higher proportion of spat during the spawning season than adult oysters, but high spat mortality resulted in a higher proportion of adult oysters in the Spring compared to the surviving spat cohort numbers (represented as one-year-old oysters).

Model simulations replicated the pattern of periodic large recruitment events as well as high mortality following recruitment events leaving a small percentage of the initial spat numbers surviving to adulthood (Fig. 7), which is similar to findings by Southworth et al. (2010b). Oysters surviving to the oldest age class (i.e., Adult+) typically lived for 4–5 years on average under the conditions presented in the model. This lifespan was older than that reported in Southworth et al. (2010b) where four-year-olds were absent in the GWR sampling sites from 2000 through 2009, however older oysters have been found on sanctuary reefs within the Great Wicomico (Schulte et al., 2009). Given that harvest and poaching occur in the natural system there is a strong likelihood of the age distribution being skewed towards younger oysters in the natural system.

The model simulated year-to-year trends in oyster density and recruitment observed in the Great Wicomico River. More specifically, the model captured the lower oyster density in 2005, followed by higher oyster density and recruitment in 2006, then higher densities in 2007–2009 that were reported by Southworth et al. (2010b).

Overall the CBOPM demonstrates the general population dynamics patterns under non-stationary environmental conditions that capture the oyster demographics, survival, mortality, and reproduction trends adequately enough to be useful for evaluating oyster population management scenarios within the Great Wicomico River.

5.4. Sensitivity analyses

Given the uncertainty associated with how the initial density of sanctuary reefs affects long term dynamics of oyster populations,

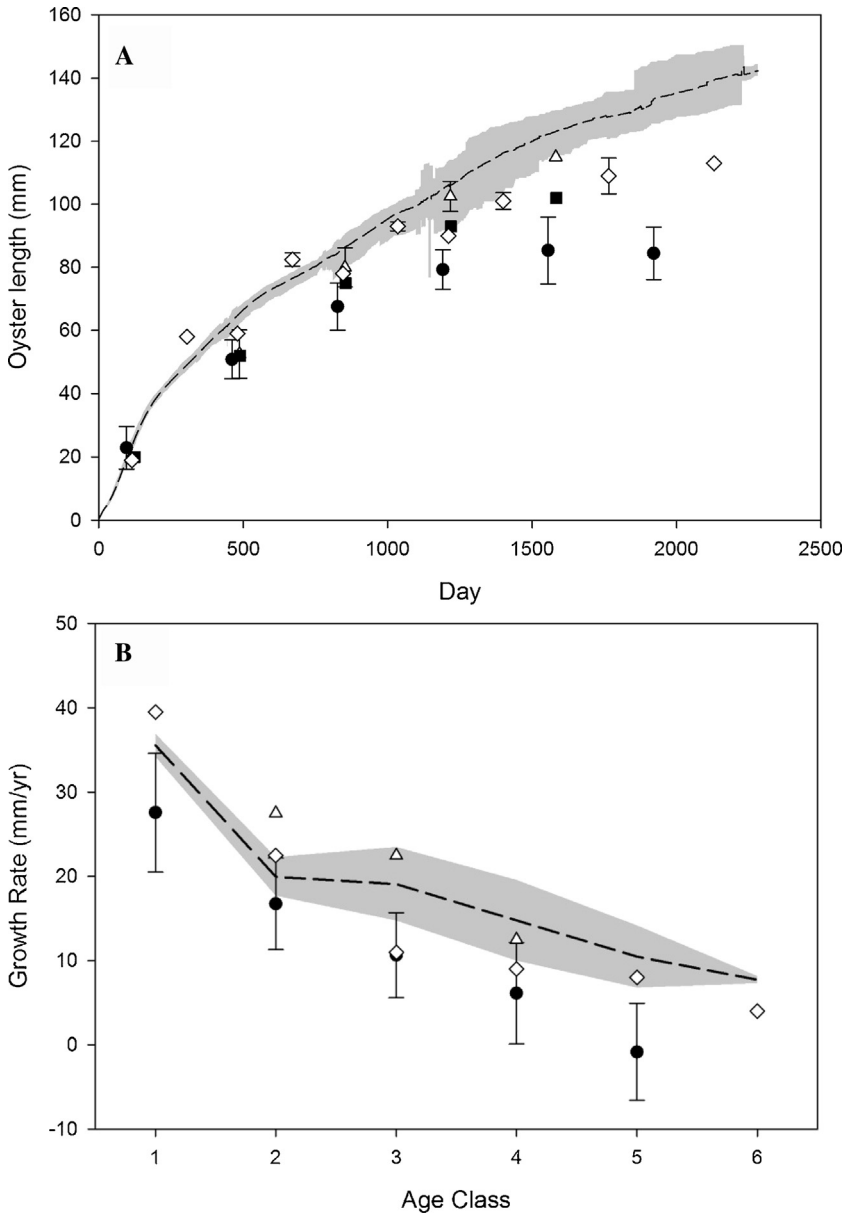

Fig. 6. Comparison of simulated results from eight year model runs (summarized over 25 stochastic replicates) to field-based studies in the Chesapeake Bay for (A) mean oyster length and (B) mean growth rate per age class. Dotted lines represent mean CBOPM results, gray areas are the minimum and maximum values obtained during the simulation. Closed circles represent data reported in Coakley (2004), open triangles (Schulte et al., 2009), open diamonds and closed squares (Southworth et al., 2010a,b). When present, error bars represent ± 1 S.D.

we performed a sensitivity analysis on initial sanctuary densities. Schulte et al. (2009) reported that sanctuaries had 4 times more oysters per square meter than non-sanctuary reefs, so under baseline conditions, we implemented the model under five initial densities (−50%, −25%, +25%, and +50% of estimates provided by Schulte et al., 2009). Further, given that our quantitative representation of density dependence is based on a simplifying assumption of linearity, we also determined how sensitive CBOPM was to changes in density-dependent fecundity by altering baseline cutoff values by −20%, −10%, +10%, and +20%.

Results from sensitivity analyses indicate that the simulated overall number of market-sized bushels was sensitive to changes in initial density of sanctuaries (Fig. 8A). As expected, decreasing the number of oysters per square meter decreased the sanctuaries contribution, via recruitment, to the system. However, the CBOPM was not that sensitive to changes in the density-dependent cut-off parameter (Fig. 8B).

6. Model application

In order to understand the long-term impacts of managing reefs as sanctuaries or as rotational harvest grounds, we used the CBOPM to project oyster dynamics using six different management scenarios. We compared oyster biomass, in terms of the number of market-sized bushels (refer to Table 9 in the supplemental material for the conversion from the numbers of oysters to bushels), by simulating system dynamics when all reefs were HR sanctuaries (HRS), LR sanctuaries (LRS), an annual harvest where each reef was LR and harvested every year (LRAH), a rotational harvest where each reef was LR and harvested once every three years (LRRH), and two combinations of HR sanctuaries and rotational harvest, which represents the current management strategies in the Great Wicomico. Specifically, we ran two scenarios exploring how spatial position of sanctuaries and harvested reefs affects system dynamics. For the first scenario, sanctuaries were placed upstream and all other reefs

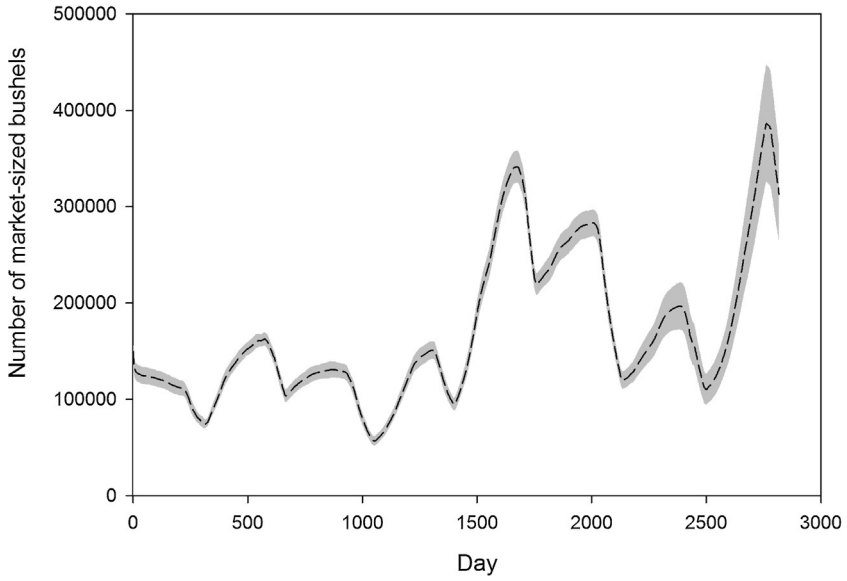

Fig. 7. Time series of the mean number of market-sized bushels (dotted line) ± 1 S.D (gray area) simulated over an 8-year period calculated from 25 stochastic replicates of the CBOPM baseline scenario.

Table 4
Description of the scenarios tested using the Chesapeake Bay Oyster Population Model (CBPOM).

Scenario abbreviation	Description	Reef type	Harvest	Harvest frequency
HRS	All reefs high-relief sanctuaries	High	N	–
LRS	All reefs low-relief sanctuaries	Low	N	–
LRAH	All low-relief harvested	Low	Y	Every reef annually
LRRH*	Low-relief rotational harvest	Low	Y	Once every 3 years
SRRH**	Mixture of Low relief/Sanctuaries reefs: 3,4,8,10, chosen randomly)	Both	Y	Low relief harvested once every 3 years
SURH**	Mixture of Low relief/Sanctuaries reefs: 1, 2, 3, & 4 all upstream)	Both	Y	Low relief harvested once every 3 years

* Three, four, and three reefs (upstream to downstream order) harvested on three year rotation starting on years 1, 2, and 3, respectively.
** Two reefs (upstream to downstream order) harvested on three year rotation beginning on years 1, 2, and 3, respectively.

were LR and were harvested once every 3 years (SURH). For the second, sanctuaries were chosen randomly and all other reefs were LR and were harvested once every 3 years (SRRH). Refer to Table 4 for complete descriptions of each scenario.

Harvesting a reef is a destructive action and there is considerable uncertainty associated with how much of a reef remains viable after a harvest event. For example, when non-market-sized oysters are put back in the water, they can get buried in sediments, which can result in mortality and reduce overall viability of the reef. In order to quantify uncertainty associated with the indirect effect of harvesting, we ran each of the harvest scenarios (LRAH, LRRH, SRRH, SURH) under three different harvest limits: (1) removing all of the reef except for 10% of the spat age class, (2) removing all of the reef except for 50% of the spat age class, and (3) removing 50% of all age classes, and leaving the remaining 50% intact. For comparative purposes, we considered the baseline condition to be the scenario where 10% of the spat age class remained after harvest. We do not suggest that this represents a typical harvesting scenario in the real system; rather, it is a point of comparison for model results.

Simulation results were summarized in terms of time series of overall number of market-sized bushels (oysters ≥76 mm). Final values of overall number of market bushels were analyzed using Analysis of Variance (ANOVA) and Bonferroni multiple comparison Post Hoc Tests to determine significant differences among scenarios ($\alpha = 0.05$).

7. Results and discussion

All of the model versions exhibited seasonal and year-to-year fluctuations in oyster abundance, typical to that observed in the field. Predictably, maximum oyster production was achieved if all oyster reefs were left as HR sanctuaries (HRS) (mean final abundance 2509,760 ± 108,368 (1 S.D.)), respectively, market-sized bushels at the end of the 8-year simulation, which was about an order of magnitude larger than the other 5 scenarios, including the LRS scenario (mean final 281,600 ± 53,786 (1 S.D.)), respectively, market-sized bushels) (Fig. 9), corroborating field results from Schulte et al. (2009) that initial density does have an impact on oyster production, and that higher density sanctuaries produce more oysters.

Under scenarios where harvesting occurred and sanctuaries were not present (LRAH & LRRH), oyster abundance trended downward over the course of the eight-year simulation, even if 50% of the reefs remained unharvested (Fig. 10). Of the six scenarios tested, the lowest oyster abundance was from the LRAH scenario, with oysters effectively being extinct within four years (Fig. 9). Lenihan and Peterson (1998) calculated that an oyster removal rate of 30% annually would result in restored reefs being completely destroyed after <4 years of harvesting, which corroborates our results. When rotational harvesting was applied to all the reefs (LRRH), the reef system did not crash, but, oyster abundance was significantly lower than the other scenarios (Fig. 9). In fact, under baseline conditions (10% of spat remain after harvest) there was not a significant difference in the final mean number of bushels between the LRAH and LRRH scenarios (Fig. 10, $P > 0.10$). Refer to Supplemental material Tables 10–21 for complete results from the statistical analyses.

Under the scenarios that reflect current management within the Great Wicomico River (SRRH & SURH), the oyster population trends fluctuated annually (as a result of inter-annual environmental conditions), but did not trend towards extinction (Fig. 9).

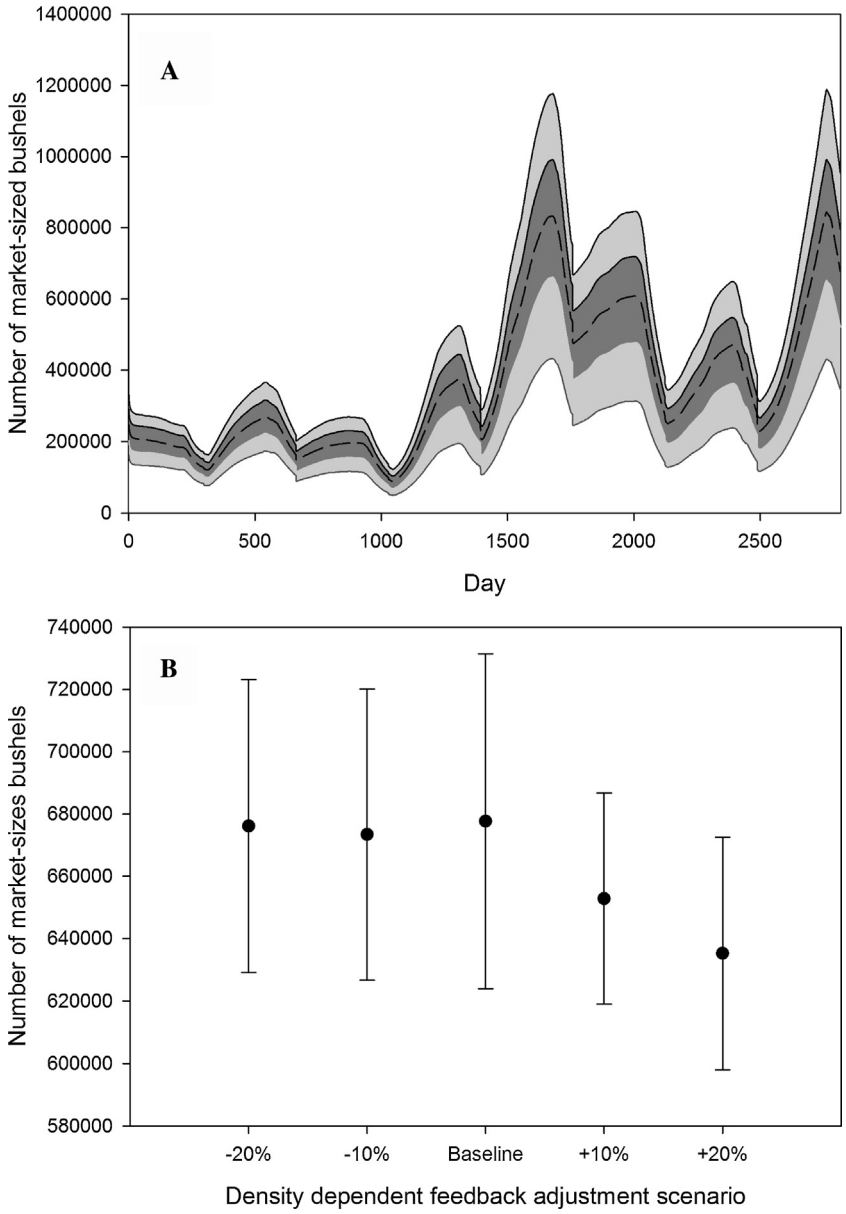

Fig. 8. Results from sensitivity analyses based on 25 stochastic replicates. (A) Comparison of changes in the number of market-sized bushels of the baseline scenario (dotted line) to scenarios when initial oyster density was increased or decreased by 50% (light gray) or 25% (Dark gray). (B) Comparison of the final number of market-sized bushels, after an eight-year simulation, of the baseline scenario (dotted line) to scenarios when the density dependent feedback factor was altered by ± 10% or 20%.

Upstream placement of sanctuaries (SURH) produced significantly fewer market-sized bushels compared to the scenario where we randomly chose sanctuary positions (SRRH) across all harvest limits (Fig. 9). For SURH, sanctuary reefs were located throughout the system (reefs 3, 4, 8, & 10, Fig. 1) rather than in a single area, and this scenario produced more oysters than all of the other scenarios, except that of HRS. The significant increase in oyster abundance emphasizes not only the importance of inter-reef recruitment but also that the spatial position of sanctuaries can positively impact oyster abundance through inter-reef recruitment. Narváez et al. (2012) indicated that larvae dispersal was variable across the Delaware Bay, with some areas being settled by larvae from other areas, while other areas were settled by larvae from their own natal reefs. Within our model domain, sanctuaries serve as sources for the harvested reefs, and provided harvested reefs with enough recruits to sustain the system. Our larval tracking model, plus that of North et al.'s (2006, 2008), showed that intra-reef recruitment is relatively low, indicating that inter-reef recruitment is crucial for sustaining oyster populations in hydrodynamically-driven systems like the Great Wicomico River. Given that inter-reef recruitment depends on hydrodynamic forcings (freshwater inflow, tidal fluctuations), it is crucial to place sanctuaries in areas where they can contribute the most recruits (Breitburg et al., 2000). Spatio-temporal variation of oyster settlement is also likely due to a combination of factors such as spatio-temporal variation in oyster fecundity and spawning success (Etherington and Eggleston, 2003; Reyns et al., 2006; Mroch et al., 2012; Narváez et al., 2012). Other models have indicated that increasing reserve (i.e., sanctuary) size disproportionately increased reserve connectivity, which can cause non-uniform dispersal of larvae throughout the system (Haase et al., 2012). Further, other models have shown that the density, age/size structure, and biomass of fishery species increases within no-take reserves in relatively short time spans (1–5 years) (Halpern and Warner, 2002; Halpern, 2003; Lester et al., 2009; Jack

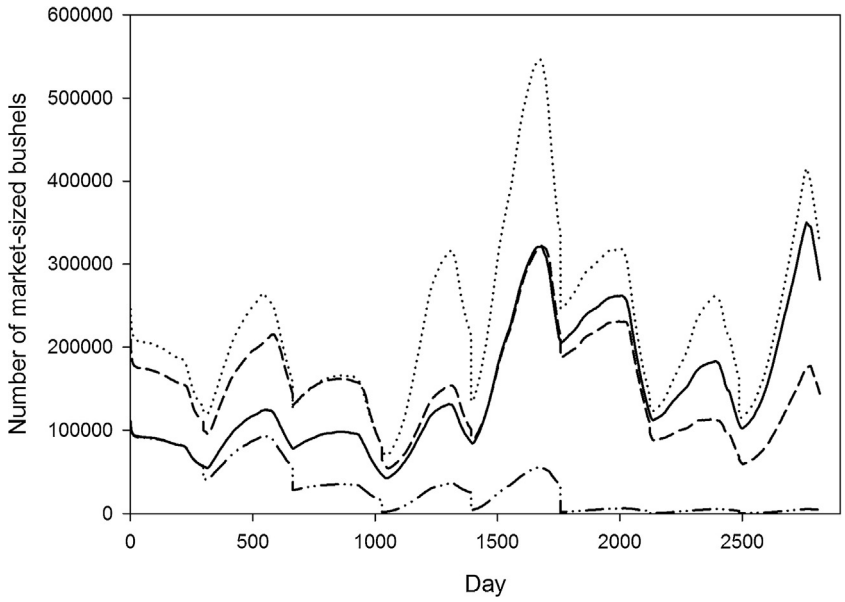

Fig. 9. Results from an 8-year time series of number of market-sized bushels for management strategies under different harvest regimes. The dotted line is the SRRH scenario with a mixture of four randomly placed sanctuary reefs and six rotationally harvested reefs; the solid line is the LRS scenario with all low-relief sanctuaries and no harvest; the dashed line is the SURH scenario: a mixture of four upstream sanctuaries and six rotationally harvested reefs; and the dotted-dashed line is the LRRH scenario with 10 rotationally harvested reefs with no sanctuaries. Rotational harvest regimes are described in more detail in Table 1. Note that the HRS and LRAH scenarios are not shown.

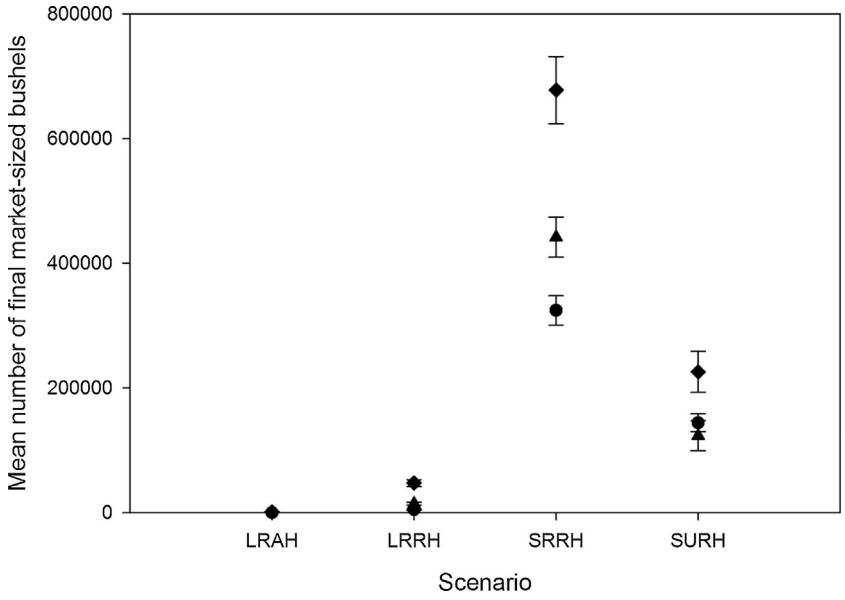

Fig. 10. Mean number of market-sized bushels at the end of an 8-year simulation (based on 25 stochastic replicates) for the four scenarios where harvest occurred, under each of three harvest limits. The circle represents 10% of the spat age class left after harvest, the triangle represents 50% of spat remain after harvest, and the diamond represents 50% of all age classes remaining after harvest. LRAH represents the low-relief annual harvest, LRRH represents the low-relief rotational harvest, SRRH represent the combination sanctuary (location chosen at random) and rotational harvest, and SURH represent the combination sanctuary (all upstream) and rotational harvest.

and Wing, 2010; Mroch et al., 2012). There have been very few studies addressing geospatial stock-recruitment relationships between parental broodstocks and local spatfall (Paynter et al., 2010).

Connectivity among reefs is crucial for adapting to climate change, and developing disease resistance (Munroe et al., 2012). Our results further emphasize the importance of connectivity in oyster metapopulations, particularly under intense harvesting pressures. Given the difficultly in tracking planktonic oyster larvae in the field, larval transport and network connectivity is a challenging issue to solve (Haase et al., 2012). Future refinement of larval tracking models should include the ability to add recruitment from outside of the system (the CBOPM only considers recruitment from the 10 modeled reefs), and the ability to simulate spat settlement outside of the modeled reefs (spat can settle on any hard substrate, but in the CBOPM larvae can only settle on the modeled reefs).

The multi-model approach that we took provides a mechanism to capture the driving force of hydrodynamics on larval transport and oyster metapopulation dynamics. Integrated models have been used to explore other aspects of oyster dynamics (Dekshenieks et al., 2000; Munroe et al., 2012; North et al., 2010; Powell et al., 2011, 2012), but their hydrodynamic models had a coarser spatial scale. The spatial scale of ADH allowed us to model the fine spatial resolution required for modeling the localized physical phenomena that affect individuals and their reefs including capturing

reef-to-reef connectivity patterns that are critical for maintaining oyster populations. Our effort revealed that larval tracking is a key component of the oyster metapopulation. In order to better understand the large-scale patterns and dynamics of oyster populations, future research should include refining and validating the PTM.

The integrated CBOPM modeling suite can be used as a tool to distinguish among multiple management scenarios, which can inform the decisions of managers and policy makers. For example, our results indicated that systems without sanctuaries produced fewer oysters. Careful thought should be placed into placement of restored reefs because different placements can confer different benefits (North et al., 2010). As with any model, these results should not be treated as dogma. Rather, these results should be used to help inform managers of potential longer-term consequences of their decisions. In addition to the aforementioned refinements to the larval tracking model, future work with the CBOPM should include exploring how re-shelling and re-seeding/broodstock placement affects the overall system-level biomass. Likewise, we made a simplifying assumption that survival rates between HR and LR were equal, however, Schulte et al. (2009) indicated that survival is higher in HR reefs. Finally, additional scenarios can be explored, primarily focusing on the temporal and spatial influence of oyster stock enhancement strategies, e.g., placement of additional high relief sanctuaries or reserve reefs, i.e., reefs that can be harvested should conditions allow for it given the current state of the system, albeit on a less frequent basis or with regard to oyster harvest size restrictions, harvest strategy restrictions, or limiting the harvest temporal window.

Oyster ecology is complex because of the biphasic life cycle and the interactions of each life stage with the physical environment. Oyster restoration and management is further complicated because it spans social, ecological, and economic boundaries. It is likely that not all of the assumptions that we included in the CBOPM will be agreed upon by other investigators in the field, but that is the nature of system dynamics modeling and the virtue by which we try to candidly put forth our assumptions so that other viewpoints can be incorporated as alternative scenarios in future research efforts. In the absence of complete datasets, multi-model integrated approaches, like the CBOPM, that embrace both ecological and socio-economic complexity, can provide managers and policy makers with much needed tools to better inform them about the long-term consequences of managing keystone ecological and economic species.

Acknowledgments

C. Cerco provided critical feedback during model development. C. Shepard and J. D. Westervelt provided code support. J. Coakley provided data for model evaluation. D. Hall, E. Lazarus, and T.W. Clumpkin provided thoughtful discussions on model development and presentation of results. This work was funded by the USACE-Norfolk District and their cost-sharing partner the Virginia Marine Resource Commission.

Appendix A. Supplementary data

Supplementary data associated with this article can be found, in the online version, at http://dx.doi.org/10.1016/j.ecolmodel.2015.03.012

References

Beck, M.W., Brumbaugh, R.D., Airoldi, L., Carranza, A., Coen, L.D., Crawford, C., Defeo, O., Edgar, G.J., Hancock, B., Kay, M.C., Lenihan, H.S., Luckenbach, M.W., Toropova, C.L., Zhang, G.F., Guo, X.M., 2011. Oyster reefs at risk and recommendations for conservation, restoration, and management. BioScience 61, 107–116.

Breitburg, D.L., Coen, L.D., Luckenbach, M.W., Mann, R., Posey, M., Wesson, J.A., 2000. Oyster reef restoration: convergence of harvest and conservation strategies. J. Shellfish Res. 19 (1), 371–377.

Cerco, C.F., Cole, T., 1993. Three-dimensional eutrophication model of Chesapeake Bay. J. Environ. Eng. 119, 1006–1025.

Chesapeake Bay Program, 1989. Chesapeake Bay Oyster Management Plan. Annapolis, MD., pp. 40.

Cloern, J.E., 2001. Our evolving conceptual model of the coastal eutrophication problem. Mar. Ecol. Prog. Ser. 210, 223–253.

Conley, D.J., 2000. Biogeochemical nutrient cycles and nutrient management strategies. Hydrobiologia 410, 87–96.

Coakley, J.M., 2004. Growth of Eastern Oyster, *Crassostrea virginica*, in Chesapeake Bay. Faculty of the Graduate School of the University of Maryland, College Park, Maryland, pp. 263 (Master of Science Thesis).

Coen, L.D., Luckenbach, M.W., Breitburg, D.L., 1999. The role of oyster reefs as essential fish habitat: a review of current knowledge and some new perspectives. Proc. Am. Fish. Soc. Symp. 22, 438–454.

Cox, C., Mann, R., 1992. Temporal and spatial changes in fecundity of Eastern oyster *Crassostrea virginica* (Gmelin, 1791) in the James River, Virginia. J. Shellfish Res. 11, 49–54.

Crockett, A., Delsouz, A., DeGregorio, J., Muhealden, A., Streicher, D., 2012. Design and analysis of a sustainable oyster aquaculture business for the West and Rhode Rivers. In: Proceedings of the 2012 IEEE Systems and Information Engineering Design Symposium. April 27, University of Virginia, Charlottesville, VA.

Danchuk, S., Wilson, C.S., 2010. Effects of shoreline sensitivity on oil spill trajectory modeling of the Lower Mississippi River. Environ. Sci. Pollut. Res. 17 (2), 331–340.

Dekshenieks, M.M., Hofmann, E.E., Klinck, J.M., Powell, E.N., 2000. Quantifying the effects of environmental change on an oyster population: a modeling study. Estuaries 23 (5), 593–610.

Dew, J.R., 2002. A Population Dynamic Model Assessing Options for Managing Eastern Oysters (*Crassostrea virginica*) and triploid Suminoe Oysters (*Crassostrea ariakensis*) in Chesapeake Bay. Virginia Polytechnic Institute, Blacksburg, Virginia, pp. 127 (Masters Thesis).

Eggleston, D.B., 1999. Application of landscape ecological principles to oyster reef habitat restoration. In: Luckenbach, M.W., Mann, R., Weston, J.A. (Eds.), Oyster Reef Habitat Restoration: A Synopsis and Synthesis of Approaches. Virginia Institute of Marine Science Press, Gloucester Point, Virginia, pp. 213–227.

Etherington, L.L., Eggleston, D.B., 2003. Spatial dynamics of large-scale, multistage crab (*Callinectes sapidus*) dispersal: determinants and consequences for recruitment. Can. J. Fish. Aquat. Sci. 60, 873–887.

Ferreira, J.G., Aguilar-Manjarrez, J., Bacher, C., Black, K., Dong, S.L., Grant, J., Hofmann, E., Kapetsky, J.M., Leung, P.S., Pastres, R., Strand, Ø., Zhu, C.B., 2010. Expert panel presentation V.3. Progressing aquaculture through virtual technology and decision making tools for novel management. In: Book of Abstracts, Global Conference on Aquaculture 2010. 22–25 September 2010, FAO/NACA/Thailand Department of Fisheries, Phuket, Thailand.

Galtsoff, P.S., 1930. The fecundity of the oyster. Science 72, 97–98.

Galtsoff, P.S., 1964. The American oyster *Crassostrea virginica* Gmelin. Fish. Bull. U.S. Fish Wildl. Serv. Bur. Comm. Fish 64, 1–480.

Gosselin, L.A., Qian, P., 1997. Juvenile mortality in benthic marine invertebrates. Mar. Ecol. Prog. Ser. 146, 265–282.

Grimm, V., Berger, U., DeAngelis, D.L., Polhill, G.J., Giske, J., Railsback, S.F., 2010. The ODD protocol: a review and first update. Ecol. Model. 221, 2760–2768.

Grimm, V., Revilla, E., Berger, U., Jeltsch, F., Mooij, W.M., Railsback, S.F., Thulke, H.-H., Weiner, J., Wiegand, T., DeAngelis, D.L., 2005. Pattern-oriented modeling of agent-based complex systems: lessons from ecology. Science 310, 987–991.

Haase, A.T., Eggleston, D.B., Luettich, R.A., Weaver, R.J., Puckett, B.J., 2012. Estuarine circulation and predicted oyster larval dispersal among a network of reserves. Estuar. Coast. Shelf Sci. 101, 33–43.

Halpern, B.S., 2003. The impact of marine reserves: do reserves work and does reserve size matter? Ecol. Appl. 13, S117–S137.

Halpern, B.S., Warner, R.R., 2002. Marine reserves have rapid and lasting effects. Ecol. Lett. 5, 361–366.

Harding, J.M., Mann, R., Southworth, M.J., Wesson, J.A., 2010. Management of the Piankatank River, Virginia, in support of oyster (*Crassostrea virginica*, Gmelin 1791) fishery repletion. J. Shellfish Res. 29, 867–888.

Horner, D., Eslinger, O., Howington, S., Ketcham, S., Peters, J., Ballard, J., 2010. Integrated high-fidelity geoscience simulations for enhanced terrain-related target detection. Comput. Sci. Eng. 12 (5), 56–63.

Hofmann, E.E., Powell, E.N., Klinck, J.M., Boyles, S., Ellis, M.S., 1994. Modeling oyster populations. II. Adult size and reproductive effort. J. Shellfish Res. 13, 165–182.

Hofmann, E.E., Powell, E.N., Klinck, J.M., Saunders, G., 1995. Modeling diseased oyster populations. I. Modeling Perkinsus marinus infections in oysters. J. Shellfish Res. 14, 121–151.

Hofmann, E.E., Powell, E.N., Klinck, J.M., Wilson, E.A., 1992. Modeling oyster populations. III. Critical feeding periods, growth and reproduction. J. Shellfish Res. 11, 399–416.

Jack, L., Wing, S.R., 2010. Maintenance of old-growth size structure and fecundity of the red rock lobster *Jasus edwardsii* among marine protected areas in Fiordland, New Zealand. Mar. Ecol. Prog. Ser. 404, 161–172.

Jackson, J.B.C., Kirby, M.X., Berger, W.H., Bjorndal, K.A., et al., 2001. Historical overfishing and the recent collapse of coastal ecosystems. Science 293, 629–638.

Kellogg, M.L., Cornwell, J.C., Owens, M.S., Paynter, K.T., 2013. Denitrification and nutrient assimilation on a restored oyster reef. Mar. Ecol. Prog. Ser. 480, 1–19.

Kennedy, V.S., Newell, R.I.E., Eble, A.F., 1996. The Eastern Oyster *Crassostrea virginica*. Maryland Sea Grant College, University of Maryland System, College Park, MD, pp. 734.
Kennedy, V.S., Krantz, L.B., 1982. Comparative gametogenic and spawning patterns of the oyster *Crassostrea virginica* Gmelin in central Chesapeake Bay. J. Shellfish Res. 2, 133–140.
Kennedy, V.S., Newell, R.I.E., Krantz, G.E., Otto, S., 1995. Reproductive capacity of the eastern oyster *Crassostrea virginica* (Gmelin) infested with the parasite *Perkinsus marinus*. Dis. Aquat. Org. 23, 135–144.
Kimmel, D.G., Newell, R.I.E., 2007. The influence of climate variation on eastern oyster (*Crassostrea virginica*) juvenile abundance in Chesapeake Bay. Limnol. Oceanogr. 52 (3), 959–965.
Kirby, M., 2004. Fishing down the coast: historical expansion and collapse of oyster fisheries along continental margins. Proc. Natl. Acad. Sci. U.S.A. 101, 13096–13099.
Lackey, T.C., Gailani, J.Z., Kim, S.-C., King, D.B., Shafer, D., 2012. Transport of resuspended dredged sediment near coral reefs at Apra Harbor, Guam. In: Proceedings of 33rd Conference of Coastal Engineering. Santander, Spain.
Lenihan, H.S., Peterson, C.H., 1998. How habitat degradation through fishery disturbance enhances impacts of hypoxia on oyster reefs. Ecol. Appl. 8, 128–140.
Lester, S.E., Halpern, B.S., Grorud-Colvert, K., Lubchenco, J., Ruttenberg, B.I., Gaines, S.D., Airame, S., Warner, R.R., 2009. Biological effects within no-take marine reserves: a global synthesis. Mar. Ecol. Prog. Ser. 384, 33–46.
Levins, R., 1969. Some demographic and genetic consequences of environmental heterogeneity for biological control. Bull. Entomol. Soc. Am. 15, 237–240.
Living Resources Subcommittee (LRSC), 2004. Draft Oyster Management Plan. Chesapeake Bay Program., pp. 43, http://www.chesapeakebay.net/
Lohse, D.P., 2002. Relative strengths of competition for space and food in a sessile filter feeder. Biol. Bull. 203, 173–180.
Malone, T.C., 1992. Effects of water column processes on dissolved oxygen, nutrients, phytoplankton and zooplankton. In: Smith, D.E., Leffler, M., Mackiernan, G. (Eds.), Oxygen Dynamics in the Chesapeake Bay. Maryland Sea Grant Publications, College Park, MD, pp. 61–112.
Mann, R., Powell, E.N., 2007. Why oyster restoration goals in the Chesapeake Bay are not and probably cannot be achieved. J. Shellfish Res. 26, 1–13.
Martin, S., Savant, G., McVan, D., 2012. Two-dimensional numerical model of the Gulf Intracoastal Waterway near New Orleans. J. Waterway, Port, Coastal, Ocean Eng. 138 (3), 236–245.
McAlpin, T., Savant, G., Brown, G., Smith, S., Chapman, R., 2013. Hydrodynamics of Knik Arm: modeling study. J. Waterway, Port, Coastal, Ocean Eng. 139 (3), 232–246.
Maryland Department of Natural Resources [DNR], 2009. Oyster Restoration and Aquaculture Development Plan, Available at (www.dnr.state.md.us/fisheries/oysters/pdfs/GovernorsOfficeSlidesFinal.pdf).
MacDonald, N.J., Davies, M.H., Zundel, A.K., Howlett, J.C., Demirbilek, Z., Gailani, J.Z., Lackey, T.C., Smith, J., 2006. PTM: Particle Tracking Model: Model theory, implementation, and example applications. In: Technical Report TR-06-20. U.S. Army Engineer Research and Development Center, Vicksburg, MS.
Moriasi, D.N., Arnold, J.G., Van Liew, M.W., Binger, R.L., Harmel, R.D., Veith, T., 2007. Model evaluation guidelines for systematic quantification of accuracy in watershed simulations. Trans. Am. Soc. Agric. Biol. Eng. 50 (3), 885–900.
Mroch III, R.M., Eggleston, D.B., Puckett, B.J., 2012. Spatio-temporal variation in oyster fecundity and reproductive output in a network of no-take reserves. J. Shellfish Res. 31 (4), 1091–1101.
Meyer, D.L., Townsend, E.C., Thayer, G.W., 1997. Stabilization and erosion control value of oyster cultch for intertidal marsh. Restor. Ecol. 5, 93–99.
Munroe, D.M., Klinck, J.M., Hofmann, E.E., Powell, E.N., 2012. The role of larval dispersal in metapopulation gene flow: local population dynamics matter. J. Mar. Res. 70 (2–3), 441–467.
Narváez, D.A., Klinck, J.M., Powell, E.N., Hofmann, E.E., Wilkin, J., Haidvogel, D.B., 2012. Modeling the dispersal of eastern oyster (*Crassostrea virginica*) larvae in Delaware Bay. J. Mar. Res. 70 (2–3), 381–409.
Newell, R.I.E., 1988. Ecological changes in Chesapeake Bay: are they the result of overharvesting the American oyster, Crassostrea virginica? In: Lynch, M.P., Krome, E.C. (Eds.), Understanding the Estuary: Advances in Chesapeake Bay Research. Chesapeake Research Consortium Publ. 129, Gloucester Point, VA, pp. 536–546.
Newell, R.I.E., 2004. Ecosystem influences of natural and cultivated populations of suspension-feeding bivalve molluscs: a review. J. Shellfish Res. 23 (1), 51–61.
Newell, R.I.E., Cornwell, J.C., Owens, M.S., 2002. Influence of simulated bivalve biodeposition and microphyrobenthos on sediment nitrogen dynamics: a laboratory study. Limnol. Oceanogr. 47, 1367–1379.
North, E.W., King, D.M., Xu, J., Hood, R.R., Newell, R.I.E., Paynter, K., Kellogg, M.L., Liddel, M.K., Boesch, D.F., 2010. Linking optimization and ecological models in a decision support tool for oyster restoration and management. Ecol. Appl. 20 (3), 851–866.
North, E.W., Schlag, Z., Hood, R.R., Li, M., Zhong, L., Gross, T., Kennedy, V.S., 2008. Vertical swimming behavior influences the dispersal of simulated oyster larvae in a coupled particle-tracking and hydrodynamic model of Chesapeake Bay. Mar. Ecol. Prog. Ser. 359, 99–115.
North, E.W., Schlag, Z., Hood, R., Zhong, L., Li, M., Gross, T., 2006. Modeling dispersal of *Crassostrea ariakensis* oyster larvae in Chesapeake Bay. In: Final report to Maryland Department of Natural Resources. Maryland Department of Natural Resources (55 p.).
Paynter, K.T., Politano, V., Lane, H.A., Allen, S.M., Meritt, D., 2010. Growth rates and prevalence of *Perkinsus marinus* prevalence in restored oyster populations in Maryland. J. Shellfish Res. 29 (2), 309–317.
Pettway, J.S., Schmidt, J.H., Stagg, A.K., 2010. Adaptive meshing in a mixed regime hydrologic simulation model. Comput. Geosci. 14 (4), 665–674.
Piazza, B.P., Banks, P.D., La Peyre, M.K., 2005. The potential for created oyster shell reefs as a sustainable shoreline protection strategy in Louisiana. Restor. Ecol. 13, 499–506.
Pouvreau, S., Bourles, Y., Lefebvre, S., Gangnery, A., Alunno-Bruscia, M., 2006. Application of a dynamic energy budget model to the Pacific oyster, *Crassostrea gigas*, reared under various environmental conditions. J. Sea Res. 56 (2), 156–167.
Posey, M., Alphin, T.D., Powell, C.M., Townsend, E., 1999. Oyster reefs as habitat for fish and decapods. In: Luckenbach, M.W., Mann, R., Weston, J.A. (Eds.), Oyster Reef Habitat Restoration: A Synopsis and Synthesis of Approaches. Virginia Institute of Marine Science Press, Gloucester Point, VA, pp. 229–238.
Powell, E.N., Klinck, J.M., Hofmann, E.E., 1996. Modeling diseased oyster populations II, Triggering mechanisms for Perkinsus marinus epizootics. J. Shellfish Res. 15, 141–165.
Powell, E.N., Hofmann, E.E., Klinck, J.M., Ray, S.M., 1992. Modeling oyster populations I. A commentary on filtration rate. Is faster always better? J. Shellfish Res. 11, 387–398.
Powell, E.N., Hofmann, E.E., Klinck, J.M., Ray, S.M., 1994. Modeling oyster populations IV: Rates of mortality, population crashes and management. Fish. Bull. 92, 347–373.
Powell, E.N., Hofmann, E.E., Klinck, J.M., Wilsonormond, E.A., Ellis, M.S., 1995. Modeling oyster populations V. Declining phytoplankton stocks and the population dynamics of American oyster (*Crassostrea virginica*) populations. Fish. Res. 24, 199–222.
Powell, E.N., Klinck, J.M., Guo, X., Ford, S.E., Bushek, D., 2011. The potential for oysters, *Crassostrea virginica*, to develop resistance to Dermo disease in the field: evaluation using a gene-based population dynamics model. J. Shellfish Res. 30 (3), 685–712.
Powell, E.N., Klinck, J.M., Guo, X., Hofmann, E.E., Ford, S.E., Bushek, D., 2012. Can oysters *Crassostrea virginica* develop resistance to dermo disease in the field: the impediment posed by climate cycles. J. Mar. Res. 70 (2–3), 309–355.
Powers, S.P., Peterson, C.H., Grabowski, J.H., Lenihan, H.S., 2009. Success of constructed oyster reefs in no-harvest sanctuaries: implications for restoration. Mar. Ecol. Prog. Ser. 389, 159–170.
Puckett, B.J., Eggleston, D.B., 2012. Oyster demographics in a network of no-take reserves: recruitment, growth, survival, and density dependence. Mar. Coast. Fish.: Dyn., Manag. Ecosyst. Sci. 4, 605–627.
Rothschild, B., Ault, J., Goulletquer, P., Heral, M., 1994. Decline of the Chesapeake Bay oyster population: a century of habitat destruction and overfishing. Mar. Ecol. Prog. Ser. 111, 29–39.
Reyns, N.B., Eggleston, D.B., Luettich, R.A., 2006. Secondary dispersal of early juvenile blue crabs within a wind-driven estuary. Limnol. Oceanogr. 51, 1982–1995.
Savant, G., Berger, R.C., 2012. Adaptive time stepping—operator splitting strategy to couple implicit numerical hydrodynamic and water quality codes. J. Environ. Eng. 138 (9), 979–984.
Schulte, D.M., Burke, R.P., Lipcius, R.N., 2009. Unprecedented restoration of a native oyster metapopulation. Science 325, 1124–1128.
Shumway, S.E., 1990. A review of the effects of algal blooms on shellfish and aquaculture. J. World Aquacult. Soc. 21, 65–104.
Shumway, S.E., 1996. Natural environmental factors. In: Kennedy, V.S., Newell, R.I.E., Eble, A.F. (Eds.), The Eastern Oyster *Crassostrea virginica*. Maryland Sea Grant College Publication, College Park, Maryland, pp. 467–513.
Smagorinsky, J., 1963. General circulation experiments with the primitive equations: I. The basic experiment. Mon. Weather Rev. 91 (3), 99–164.
Southworth, M.J., Harding, J.M., Mann, R., 2006. The Status of Virginia's Public Oyster Resource 2005. Virginia Institute of Marine Science, Gloucester Point, Virginia, pp. 49.
Southworth, M.J., Harding, J.M., Mann, R., 2007. The Status of Virginia's Public Oyster Resource 2006. Virginia Institute of Marine Science, Gloucester Point, VA, pp. 49.
Southworth, M.J., Harding, J.M., Mann, R., 2008. The Status of Virginia's Public Oyster Resource 2007. Virginia Institute of Marine Science, Gloucester Point, VA, pp. 49.
Southworth, M.J., Harding, J.M., Mann, R., 2009. The Status of Virginia's Public Oyster Resource 2008. Virginia Institute of Marine Science, Gloucester Point, VA, pp. 53.
Southworth, M.J., Harding, J.M., Mann, R., 2010a. The Status of Virginia's Public Oyster Resource 2009. Virginia Institute of Marine Science, Gloucester Point, VA, pp. 52.
Southworth, M., Harding, J.M., Wesson, J.A., Mann, R., 2010b. Oyster (*Crassostrea virginica*, Gmelin 1791) population dynamics on public reefs in the Great Wicomico River, Virginia, USA. J. Shellfish Res. 29 (2), 271–290.
Southworth, M.J., Harding, J.M., Mann, R., 2011. The Status of Virginia's Public Oyster Resource 2010. Virginia Institute of Marine Science, Gloucester Point, VA, pp. 50.
Southworth, M.J., Harding, J.M., Mann, R., 2012. The Status of Virginia's Public Oyster Resource 2011. Virginia Institute of Marine Science, Gloucester Point, VA, pp. 51.
Tate, J.N., Lackey, T.C., McAlpin, T.O., 2010. Seabrook Fish Larval Transport Study Technical Report TR-10-12. U.S. Army Engineer Research and Development Center, Vicksburg, MS.
Tate, J., Savant, G., McVan, D., 2012. Rapid response numerical modeling of the 2010 Pakistan flooding. Leadersh. Manage. Eng. 12 (4), 315–323.
Teeter, A.M., Johnson, B.H., Berger, C., Stelling, G., Scheffner, N.W., Garcia, M.H., Parchure, T.M., 2001. Hydrodynamic and sediment transport modeling with emphasis on shallow-water, vegetated areas (lakes, reservoirs, estuaries and lagoons). Hydrobiologia 444 (1–3), 1–23.

Tolley, S.G., Volety, A.K., 2005. The role of oysters in habitat use of oyster reefs by resident fishes and decapod crustaceans. J. Shellfish Res. 24, 1007–1012.

Vogel, R.M., Wilson, I.W., Daly, C., 1999. Regional Regression Models of Annual Stream Flow for the United States. J. Irrig. Drain. Eng. 125 (3), 148–157.

Volety, A.K., Savarese, M., Tolley, S.G., Arnold, W., Sime, P., Goodman, P., Chamberlain, R., Doering, P.H., 2009. Eastern oysters (*Crassostrea virginica*) as an indicator for restoration of Everglades' ecosystems. Ecol. Indic. 9 (Suppl. 6), S120–S136.

Volstad, J.H., Christman, M.C., Lewis, D., Weber, E.D., Dew, J., 2007. Appendix A: a demographic model of oyster populations in the Chesapeake Bay to evaluate proposed oyster-restoration alternatives. In: Banta, T.R., DeLisle, C., Donovan, C., Humbles, T., Meade, C. (Eds.), U.S. Army Corps of Engineers, Norfolk District, Norfolk, VA. Final programmatic environmental impact statement for oyster restoration in Chesapeake Bay including the use of a native and/or nonnative oyster, June 2009. , 250 pp.

Wang, H., Huang, W., Harwell, M.A., Edmiston, L., Johnson, E., Hsieh, P., Milla, K., Christensen, J., Stewart, J., Liu, X., 2008. Modeling oyster growth rate by coupling oyster population and hydrodynamic models for Apalachicola Bay, Florida, USA. Ecol. Mod. 211 (1–2), 77–89.

Whyte, J.N.C., Englar, J.R., Carswell, B.L., 1990. Biochemical composition and energy reserves in *Crassostrea gigas* exposed to different levels of nutrition. Aquaculture 90, 157–172.

Wilberg, M.J., Livings, M.E., Barkman, J.S., Morris, B.T., Robinson, J.M., 2011. Overfishing, disease, habitat loss, and potential extirpation of oysters in upper Chesapeake Bay. Mar. Ecol. Prog. Ser. 436, 131–144, http://dx.doi.org/10.3354/meps09161

Wilensky, U., 1999. NetLogo. Center for Connected Learning and Computer-Based Modeling, Northwestern University, Evanston, IL, ⟨http://ccl.northwestern.edu/netlogo/⟩.